NASA CONTRACTOR REPORT

NASA CR-214

ANALYTICAL STUDY OF MODERATOR WALL COOLING OF GASEOUS NUCLEAR ROCKET ENGINES

by G. H. McLafferty

Prepared under Contract No. NASw-847 *by*
UNITED AIRCRAFT CORPORATION
East Hartford, Conn.
for

NATIONAL AERONAUTICS AND SPACE ADMINISTRATION • WASHINGTON, D. C. • APRIL 1965

NASA CR-214

ANALYTICAL STUDY OF MODERATOR WALL COOLING OF GASEOUS NUCLEAR ROCKET ENGINES

By G. H. McLafferty

Prepared under Contract No. NASw-847 by
UNITED AIRCRAFT CORPORATION
East Hartford, Conn.

for

NATIONAL AERONAUTICS AND SPACE ADMINISTRATION

For sale by the Office of Technical Services, Department of Commerce,
Washington, D.C. 20230 -- Price $3.00

Analytical Study of Moderator Wall Cooling

of Gaseous Nuclear Rocket Engines

TABLE OF CONTENTS

TABLE OF CONTENTS (cont'd)

Analytical Study of Moderator Wall Cooling of Gaseous Nuclear Rocket Engines

SUMMARY

An analytical study was conducted to investigate cooling problems in high-thrust cavity-type gaseous nuclear rocket engines resulting from (a) heat deposition within the interior of the moderator-reflector surrounding the cavity by neutrons and gamma rays and (b) heat deposition on the surface of the cavity by fission fragments, beta particles, radiant heat transfer, and convection. The study included determination of the size and spacing of coolant tube passages required in the wall of the moderator-reflector and the pressure drop of the coolant fluid in these passages. A number of different coolant flow cycles were considered.

The results of the study indicate that more heat will be deposited in the interior of the moderator than on the surface of the cavity, but that the heat deposited on the surface of the cavity may be more difficult to remove. Removal of the energy deposited in the interior of the moderator will require the use of a large number of small-diameter coolant passages. The major causes of cavity surface heating will be beta-particle impingement and thermal radiation, but calculations indicate that heating by beta-particle impingement can be reduced by the use of a magnetic field and that heating by thermal radiation can be reduced by the use of seeds in the propellant.

In addition to a description of the moderator cooling study in the main body of the report, three additional studies are described in the appendices: determination of the fuel-containment characteristics of a gaseous nuclear rocket in which no attempt is made to separate propellant and fuel; determination of the effect of different propellants on the specific impulse of gaseous nuclear rockets; and a description of a facility concept which might be employed for testing gaseous nuclear rockets.

CONCLUSIONS

1. Beta-particle heating of the cavity surface of high-thrust cavity-type gaseous nuclear rocket engines will require either the use of a magnetic field (approximately 1000 gauss for an engine having a thrust-to-weight ratio of 20) to reduce the heating rate to acceptable values or the use of a porous wall with closely-spaced pores to permit the heat deposited to be conducted through the wall material to the coolant fluid passing through the pores.

2. A uniformly distributed seed will be required in high-thrust cavity-type gaseous nuclear rocket engines to prevent excessive heating of the cavity surface by thermal radiation (seed density on the order of 1 percent of propellant mass density for an engine thrust-to-weight ratio of 20 and a pressure level of 1000 atm; required seed density fraction is inversely proportional to pressure).

3. Removal of heat deposited within the interior of the moderator of gaseous nuclear rocket engines by neutrons and gamma rays will require the use of a large number of small-diameter coolant passages (void fraction of approximately 5 percent and 0.020 in.-dia passages for an engine thrust-to-weight ratio of 20 and a pressure level of 1000 atm; resulting pressure drop of approximately 10 atm is inversely proportional to absolute pressure).

4. The following will be reduced by the use of an auxiliary coolant loop and heat exchanger to transfer heat from the moderator to the propellant:

   a. Pressure differences and resultant stresses in the moderator caused by the turbopump cycle.

   b. Neutron absorption caused by the presence of hydrogen coolant in the moderator.

   c. Chemical attack of hydrogen on the moderator wall.

5. The flow patterns within the cavity of a high-thrust cavity-type gaseous nuclear rocket must be designed so that the temperature difference across the boundary layer which governs convective heat transfer to the wall is minimized.

INTRODUCTION

It has been known for many years that the limitation on the specific impulse of a solid-core nuclear rocket imposed by allowable maximum material temperatures can be circumvented by employing the nuclear fuel in gaseous form. It is theoretically

possible in such gaseous nuclear rocket engines to attain rocket exhaust temperatures on the order of 25,000 R which, in conjunction with the use of hydrogen propellant, will lead to a specific impulse of approximately 2500 sec for a nozzle efficiency of 80 percent. It is also theoretically possible to attain engine thrust-to-weight ratios substantially greater than unity in gaseous nuclear rockets. The primary problem which must be overcome before gaseous nuclear rockets become feasible is that of transfer of energy to the propellant without causing an unacceptable loss of expensive nuclear fuel. Attempts to solve this problem have lead to the formulation of many different gaseous nuclear rocket concepts. For the present purpose it is convenient to divide these concepts into two categories: those employing cavity reactors and those employing homogenous reactors. The cavity reactor employs a single cavity for the high-temperature gases and is exemplified by the coaxial-flow reactor of Ref. 1. The homogenous reactor employs a large number of individual cavities within the reactor and is exemplified by the multi-unit vortex configuration of Ref. 2. A typical homogenous reactor may employ 10^4 individual cavities and, for the same total cavity volume, may have 10^2 times as much cavity surface area as a cavity reactor.

Approximately 90 percent of the energy created in both cavity and homogenous reactors is deposited in the gases within the reactor, while the remaining 10 percent is deposited in the walls of the reactor. This 10 percent of the energy is deposited both on the surface of the reactor cavities and within the interior of the moderator walls surrounding the cavities. In a homogenous reactor, the energy deposition within the interior of the moderator walls is approximately uniform, while in a cavity reactor the energy deposition within the moderator walls is concentrated near the surface of the cavity. The energy deposited on the surface of the walls per unit area is much less for the homogenous reactor than for the cavity reactor because of the increased surface area of the former. Therefore, the problem of removing heat from both the interior and the surface of the moderator walls is greater for a cavity reactor than for a homogenous reactor. For this reason, the analysis of the present report was directed towards investigating the moderator coolant problems of cavity reactors.

The thrust-to-weight ratio of both solid-core and gaseous-core nuclear rocket engines is limited by the rate at which heat can be removed from the solid walls of the engine configuration. Although many analyses have been conducted to investigate heat transfer rates in solid-core nuclear rocket engines, no studies are available concerning heat transfer rates and resulting limitations on engine thrust for gaseous nuclear rocket engines. Therefore, the analysis described in the following sections was initiated to obtain information concerning limitations on engine thrust characteristics which might be caused by the problem of moderator wall cooling.

HEAT DEPOSITION RATES IN MODERATOR WALL

The location of a moderator-reflector in a possible gaseous nuclear rocket engine configuration is shown in Fig. 1. Although insufficient information is available from studies of various gaseous nuclear rocket concepts to fix the dimensions and materials of this moderator, it is convenient to adopt a reference configuration so that a feeling may be developed for the quantitative values of the parameters which describe the characteristics of the engine. The characteristics of this reference engine configuration are shown in Fig. 2. The total engine weight of 300,000 lb was obtained by adding weight to the weight of the moderator to allow for the pressure shell, the exhaust nozzle, the turbopump system, and any external heat exchanger required. The exit enthalpy corresponding to the specific impulse of 2500 sec was determined such that the exhaust velocity corresponding to the specific impulse was equal to 80 percent of the exhaust velocity resulting from conversion of all of the propellant energy to kinetic energy. The absolute power level for the reference engine configuration was chosen to provide a thrust-to-weight ratio of approximately 20.

Information from Ref. 3 on the energy release in the form of neutrons, gamma rays, fission fragments, and beta particles due to fission of plutonium-239 is given in Table I for times after fission of 5 and 100 sec (i.e., for fission product residence times in a gaseous nuclear rocket of 5 and 100 sec). Calculations of the energy deposition in the moderator wall from each of these forms of energy release and from thermal radiation and convection from gases heated by this energy is given in the following subsections. A summary of this information is also given in Table II. It should be emphasized that the results shown in Table II are based on specific assumptions of engine configuration and that exact determination of the heat deposition rates requires complete specification of the geometry and conditions within the engine.

Fission Fragment Heating

It can be seen from Table I that most of the energy created in the fission process appears in the form of fission fragments. According to the formula on p.321 of Ref. 4, the range of a fission fragment in hydrogen at a pressure of 500 atm and a temperature of 10,000 R is approximately 0.2 in. Therefore, direct heating of the walls by fission fragments can be eliminated if a gas film containing no nuclear fuel and having a thickness of 0.2 in. or greater can be placed between the region containing gaseous nuclear fuel and the wall of the cavity. If any nuclear fuel were located less than one fission fragment distance from the cavity wall, the energy deposited in the wall would be released in a very thin layer near the wall surface. It is assumed in this report that the energy deposition on the surface of the wall by fission fragments is negligible. It should be noted, however, that energy created

by fission fragments can cause wall heating as a result of convection or radiation of energy from gas heated by the fission fragments (see following subsections).

Neutron and Gamma Ray Heating

Calculations to determine the attenuation of neutron and gamma ray energy by hydrogen gas at a pressure of 500 atm and a temperature of 10,000 R indicate that a one-ft-thick layer of this gas would attenuate less than one percent of the gamma ray energy and approximately 5 percent of the energy from fast neutrons. This energy absorption is so small that it is assumed in the following calculations that all energy appearing in the form of neutrons and gamma rays will impinge on the wall of the moderator-reflector.

The energy flow and energy deposition rate in a graphite moderator due to neutrons and gamma rays is shown in Fig. 3 as a function of the distance from the inside surface of the moderator. The curves shown in this figure were obtained from Ref. 5 and apply to the case of a source of neutrons and gamma rays located along the centerline of a cylinder having a length equal to the cavity diameter. The energy deposited in a given volume is determined by the difference between the energy flow entering and leaving the volume. It can be seen from Fig. 3 that the maximum energy deposition rate occurs at the inside surface of the moderator, and falls off approximately exponentially with distance. The attenuation factor in this exponent according to Fig. 3 is approximately 1.57 ft^{-1}. Therefore, for a neutron and gamma ray flux approaching the inside surface of the moderator-reflector of 70,000 to 78,000 $BTU/sec\text{-}ft^2$ (see Table I), the energy deposition rate near the inside surface of the moderator would be from 110,000 to 122,000 $BTU/sec\text{-}ft^3$. This range of energy deposition rates is shown in the summary in Table II.

Data from Ref. 5 showing the variation of energy flow due to neutrons and gamma rays with distance for three different moderator materials is given in Fig. 4. The energy flow in a heavy-water moderator falls off initially at approximately the same rate as in a graphite moderator and, therefore, the energy deposition rates would be approximately the same as for a graphite moderator. However, the energy flow in a beryllium-oxide moderator falls off approximately twice as fast as in a graphite moderator. Therefore, the energy deposition rate at the inside surface of a beryllium-oxide moderator-reflector would be approximately twice that shown in Table II for a graphite moderator-reflector.

Beta-Particle Heating

Beta particles from the nuclear fission process would lose approximately 25 percent of their energy in passing through a one-ft-thick layer of hydrogen at a pressure of 500 atm and a temperature of 10,000 R. Since the beta particles would also lose some of their energy in passing through the fuel region, it has been arbitrarily

assumed that 50 percent of the energy created in the form of beta particles would be incident on the cavity wall. This energy would be deposited in a very thin layer on the inside surface of this wall (approximately half of energy in distance of 0.01 in.) rather than being deposited within the interior wall volume as in the case of neutron and gamma energy. Therefore, the absolute energy deposited on the surface of the wall from beta particles is from approximately 6000 to 16,000 BTU/sec-ft^2 for the reference engine (see summary in Table II).

It will be shown in a following subsection that surface heat deposition rates of the magnitude which may be caused by beta particle impingement will be very difficult to remove by regenerative cooling. One possible method of reducing beta particle heating of the wall is to employ a magnetic field in the cavity to cause the beta particles to spiral around the magnetic field lines until their energy is lost by collisions with hydrogen and fuel. Calculations which include allowance for the relativistic mass of the beta particles indicate that the radius of curvature of a typical beta particle having an energy of 2 Mev is approximately 3 in. for a magnetic field strength of 1000 gauss. In such a magnetic field, the only beta particles which have any chance of striking the wall would be those which originated from fissions occurring within two radii or approximately 6 in. of the wall. For the reference engine of Fig. 2, approximately 27 percent of the cavity volume is located within 6 in. of the cavity wall. However, the fraction of the beta particle energy deposited on the wall would be considerably less than 27 percent for three reasons. First, a large percentage of the beta particles would spiral in a path which would not intersect the wall. Second, the beta particles would lose a portion of their energy in passing through the gases within the reactor, and hence their radii of curvature would be reduced. Third, it may be possible to design the gaseous nuclear rocket such that the local density of nuclear fuel within 6 in. of the cavity walls is considerably less than the density of the nuclear fuel in the center of the reactor. In consideration of these factors, it has been assumed that between one and four percent of the energy created by the beta particles would impinge on the cavity wall for configurations employing a magnetic field within the cavity having a strength of approximately 1000 gauss. For the reference engine, the energy deposition on the wall surface would be between 120 and 1200 BTU/sec-ft^2 (see Table II). More accurate determination of wall surface heating by beta particles requires examination of specific gaseous nuclear rocket configurations.

Creation of a magnetic field having a strength of 1000 gauss would require shaft power from the turbopump system and would result in added weight due to field coils, an electric generator, and changes in the turbopump system. It was assumed in calculating these penalties that the copper coils could be maintained at a temperature of 40 K by hydrogen cooling in order to minimize the electrical resistance of the copper. These coils would probably be mounted outside of the pressure shell surrounding the moderator in order to minimize the heating of the coils by nuclear radiation. The cylindrical region inside of the magnetic field coils was assumed to have a diameter of 15 ft and a length of 15 ft. If the total weight of the copper coils employed were 500 lb, approximately 250 kw of electrical energy would be

required to create a magnetic field of 1000 gauss inside this cylindrical region. The shaft power taken from the turbopump assembly to provide this electric power would represent less than 0.1 percent of the pump power for the reference engine and would require almost no increase in turbopump weight. However, a penalty of approximately 2 lb/kw would have to be paid to provide the electrical generator necessary to convert the shaft power to electric power. Thus, the weight of this generator would be approximately 500 lb, and the total weight associated with creating a magnetic field of 1000 gauss would be approximately 1000 lb. It would be desirable to shape the magnetic field to provide a magnetic bottle within the cavity in order to prevent heating of the end walls as well as heating of the cylindrical walls. Although creation of such a shaped magnetic field would result in some increase in weight, the uncertainty in engine configuration does not warrant inclusion of the required refinement in the procedure for estimating weight. Therefore, the estimated weight of 1000 lb associated with minimizing wall heating by beta particles is probably of the correct order of magnitude.

Radiant Heat Transfer to Wall

Although pure hydrogen is transparent to thermal radiation in the visible portion of the spectrum at low temperatures (Refs. 6 and 7), it can be seeded with small particles to cause absorption of thermal radiation from hot regions in the reactor before this radiation impinges on the cavity wall. Calculations of the opacity of small particles using the Mie theory are reported in Ref. 8 and measurements of the opacity of small particles are reported in Refs. 9, 10, and 11. The tests reported in Ref. 11 employed aerodynamic shear to break up particle agglomerates which are believed to have been the cause of low measured particle opacities in the tests reported in Ref. 9. The measurements reported in Ref. 11 indicate an extinction parameter, b_e, of approximately 55,000 cm^2/gm for graphite particles and approximately 8000 cm^2/gm for tungsten particles. These measured values of extinction parameter are approximately 80 percent of the theoretical values from Ref. 8 for a particle diameter of 0.1 microns and a wavelength of 0.55 microns. It is not possible to employ graphite particles in a gaseous nuclear reactor because of the resulting reaction of graphite and hydrogen at high temperatures (see Ref. 12). Therefore, it is necessary to employ a material such as tungsten which will not react with the propellant.

A series of calculations have been made to determine the thickness of hydrogen layer (seeded with tungsten) required to attenuate incident thermal radiation by a factor of 1000. The results of these calculations, which are given in Fig. 5, were determined on the basis of an attenuation parameter of 8000 cm^2/gm (see preceding paragraph), a particle seed mass density of one percent of the hydrogen mass density, and the hydrogen densities given in Refs. 6 and 7. It can be seen from Fig. 5 that the thickness of the seeded hydrogen layer which will result in a reduction in thermal radiation by a factor of 1000 for a hydrogen pressure of 1000 atm is from 3 to 6 in.

Determination of the magnitude of the thermal radiant energy approaching the seeded hydrogen layer requires detailed knowledge of the conditions existing within the reactor cavity. For reactor configurations similar to the coaxial flow reactor of Ref. 1, it is possible that the total radiant energy approaching the seeded hydrogen layer might be equal to the energy created within the fuel region by fission fragments and beta particles. This radiant energy would represent approximately 90 percent of the total energy released or approximately 900,000 BTU/sec-ft^2 for the reference engine of Fig. 2. An alternate method of calculation would be to assume that the radiant energy incident upon the seeded hydrogen layer is equal to black-body radiation corresponding to the desired propellant temperatures. For a specific impulse of 2500 sec, the required average propellant temperature is approximately 22,000 R and the corresponding black-body radiation intensity is approximately 112,000 BTU/sec-ft^2. Attenuation of these incident radiant energies by a factor of 1000 would result in heat deposition on the surface of the wall of 100 to 900 BTU/sec-ft^2 (assuming a wall absorptivity of unity). Further reductions in thermal radiant energy incident on the wall can obviously be attained by the use of thicker layers of seeded gas or by an increase in the density of the particle seeds. It should be noted, however, that it is extremely important that this particle seed be uniformly distributed throughout the hydrogen layer, since local regions of low seed density would result in extreme local overheating of the cavity wall.

It is also necessary to account for re-radiation from the particle seeds to the wall as well as to account for the fraction of incident radiant energy passing through the seed blanket. If an effective seed radiating temperature of 7000 R and a wall temperature of 5000 R are assumed, the black-body heat transfer rate to the wall would be approximately 850 BTU/sec-ft^2.

The range of surface heat deposition rates for the reference engine due to thermal radiation noted in Table II was set at 200 to 2000 BTU/sec-ft^2 on the basis of the discussion in the preceding paragraphs. Refinement of these estimates requires calculation of the spectral heat flux for specified temperature distributions, spectral seed opacities and spectral wall absorptivities.

Convective Heat Transfer to Wall

The convective transfer of heat from the hot gases within the cavity of a gaseous nuclear rocket to the walls of the cavity is determined by the details of the velocity and temperature distributions within the cavity. It is assumed in the following calculations that a relatively cool region of gas exists between the cavity walls and the very hot regions within the cavity. The corresponding temperature distribution is indicated in Fig. 6. It is assumed that the velocity and temperature boundary layers are confined to this region of relatively cool gases near the chamber wall. The heat transfer to the wall is then determined by the conditions at the outside edge of the boundary layer indicated in Fig. 6. This rate of heat transfer is governed by the following equation.

$$\left(\frac{Q}{A}\right)_{CONVECTION} = St\,\rho_o V_o C_p (T_{GAS} - T_{WC}) \qquad (1)$$

The nomenclature in the preceding equation is defined in the List of Symbols.

Typical curves showing the effect of gas temperature and velocity on the convective heat transfer to a cavity wall determined from Eq. (1) are shown in Fig. 7. The Stanton number of 0.0012 employed in the calculations is typical of those which are encountered at moderate Reynolds numbers. Note that results are shown for hydrogen temperatures both lower and higher than the assumed wall temperature of 5000 R. A range of values from -2000 to +3000 BTU/sec-ft^2 has been selected from Fig. 7 for use in Table II. The convective heat transfer rate is approximately proportional to hydrogen pressure for values other than the value of 500 atm used in the calculation in Fig. 7.

MODERATOR COOLANT FLOW CYCLES

The cooling ducts in the moderator-reflector of a gaseous nuclear rocket engine must be positioned so as to remove both the heat deposited on the internal surface of the moderator and the heat deposited within the interior of the moderator. Because the heat deposited on the surface is a small fraction of the total heat which must be removed from the moderator, this surface heating is neglected in the general discussion of coolant flow cycles in the following subsections. However, it is shown in the section entitled DETAILS OF COOLANT FLOW CHARACTERISTICS that the problem of removing the heat deposited on the internal surface may be more restrictive in terms of local allowable moderator material thicknesses than that imposed by the heat deposited within the interior of the moderator.

Cycle with Inward Coolant Flow

Direct Cooling with Propellant Flow

The coolant flow cycle usually considered for application to gaseous nuclear rockets is shown in Fig. 8a and in Fig. 1. (The coolant cycles shown in Figs. 8b and 8c will be discussed in following subsections.) The wavy duct shape within the moderator shown in Fig. 8a indicates a large number of small-diameter coolant passages. A discussion of the required diameter and spacing of these coolant passages is given in the section entitled DETAILS OF COOLANT FLOW CHARACTERISTICS. The straight ducts shown passing through the moderator in Fig. 8a would be relatively

large ducts (on the order of one in. in diameter) and hence, because of their small surface area, would remove a very small portion of the heat deposited in the moderator by neutron and gamma interactions. Also, because of the large diameter of these ducts relative to the diameter of the coolant passages, the volume fraction devoted to these ducts for a given pressure drop would be much less than for the coolant passages.

The relative pressures in different portions of the cycle shown in Figs. 1 and 8a are governed to a large extent by the characteristics of the thermodynamic cycle associated with the turbopump system. This thermodynamic cycle has been analyzed using two different techniques for calculating the turbine characteristics: a perfect-gas expansion through the turbine assuming a ratio of specific heats of 1.4 and a value of specific heat at constant pressure of 4.0 BTU/lb-deg R; and a real-gas expansion through the turbine using the Mollier diagram in Ref. 13. In both calculation procedures it was assumed that: the turbine inlet temperature was 2200 R; the turbine efficiency was 85 percent; the pump efficiency was 80 percent; and the pump characteristics could be calculated from the product of specific volume and pump pressure rise using a hydrogen density of 4.43 lb/ft^3. For reference, the work required to provide a pump exit pressure of 1000 atm is 769 BTU/lb. For the reference engine of Fig. 2, the resulting pump power would be 2.55×10^6 hp.

The results of calculation of the turbopump cycle characteristics are given in Fig. 9. The two different methods of calculating turbine characteristics give essentially identical results up to a turbine exit pressure of approximately 600 atm. However, the turbine pressure drop for turbine exit pressures higher than 600 atm as indicated by the perfect-gas calculations is substantially greater than that indicated by the real-gas calculations. It will be shown in the section entitled DETAILS OF COOLANT FLOW CHARACTERISTICS that the heat exchanger pressure drops are on the order of one percent of the absolute pressure. Therefore, the differences in turbine pressure drop resulting from changes in the heat exchanger pressure drop is relatively small. At high values of turbine exit pressure, the effect of changes in the characteristics of the heat exchanger located between the pump and the turbine is much less than the difference between the results calculated for a perfect-gas turbine expansion and a real-gas turbine expansion. It should be pointed out that the Mollier diagram from Ref. 13 which was employed in the real-gas expansion calculation is based on an extensive extrapolation of available data and hence may be substantially in error. Additional information on the characteristics of hydrogen at the conditions which might exist at the entrance to the turbine are badly needed.

The energy flow curves given in Figs. 3 and 4 determine the variation of hydrogen coolant temperature with distance from the inside surface of the moderator. An example of such a variation for inward coolant flow is given by the solid curve in Fig. 10. For values of $r - r_1$ less than 0.6 ft, the temperature in Fig. 6 is proportional to the energy flow curve for a radius of 5 ft given in Fig. 3. The temperatures at values of $r - r_1$ greater than 0.6 ft were adjusted upward by approximately 150 deg to account for the temperature drop in the turbine required to drive the

pump. For the assumed pressure of approximately 500 atm at values of $X < 0.6$ ft, the pressure drop through the turbine according to Fig. 9 would be approximately 130 atm. A discussion of methods of avoiding this pressure drop within the moderator is given in the following subsection.

Although the hydrogen temperature distribution is determined by the energy deposition due to neutrons and gamma rays, the temperature distribution in the moderator is determined by a number of different design variables. For instance, it is possible to obtain a moderator temperature distribution such as that shown in Curve A of Fig. 10 in which the difference in temperature between the moderator and the hydrogen coolant is independent of distance through the moderator. Such a temperature distribution in the moderator could be determined by proper selection of the variation of coolant passage diameter with distance through the moderator. It may also be desirable to select a moderator temperature distribution such as that given by Curve B in Fig. 10. This curve indicates a high moderator temperature at all positions within the moderator-reflector and results in the maximum temperature difference between the wall of the coolant tubes and the hydrogen coolant. Such a temperature distribution would minimize the required pressure drop in the moderator for a given diameter and spacing of coolant passages.

Various studies have indicated that beryllium oxide, which is a superior moderator material to graphite for small engine sizes, loses structural strength above a temperature on the order of 3000 R. It can be seen from Fig. 10 that the temperature distribution indicated by Curve A would permit use of a beryllium oxide moderator at distances from the inside surface of the moderator-reflector greater than approximately 0.38 ft. It is also desirable to employ heavy water as a moderator for regions in which the temperature is below that which would result in significant decreases in heavy-water density. If this temperature is selected as 1000 R, it can be seen from Fig. 10 that it is permissible to employ heavy water at values of $r - r_1$ greater than approximately 1.5 ft. It is very desirable to employ heavy water in as large a portion of the moderator as possible since studies have indicated that the use of pure heavy water (if it can be cooled properly) in all portions of the moderator would result in critical fuel densities between 1/3 and 1/10 of those required for graphite or beryllium oxide moderators.

Coolant temperature distributions in moderators with inward coolant flow are shown in Fig. 11 for maximum coolant temperatures of 5000 and 3000 R. These temperature distributions were calculated by neglecting the temperature drop through the turbine circuit. It was assumed in constructing the curves that the maximum permissible temperature for the heavy-water portions of the moderator was 1000 R and that the maximum permissible temperature for the BeO portions of the moderator was 3000 R. In Fig. 11 portions of the moderator composed of graphite are indicated by solid curves, the portions composed of BeO by dashed curves, and the portions composed of heavy water by dash-dot-dash curves.

The temperatures indicated in Fig. 11 by the curves constructed for a single moderator material (i.e., Curve A for maximum coolant temperatures of 5000 and 3000 R and Curve C for a maximum coolant temperature of 3000 R) are directly proportional to the corresponding heat flows in Fig. 4. The curves for composite moderators (i.e., those made up of two or more different moderator materials) were obtained from curves similar to those in Fig. 4 with the exponential heat flow decay in each portion of the moderator matched to the heat flow decay from adjacent portions of the moderator. It can be seen from Fig. 11 that the BeO portion of the moderator can be initiated at X = 0 for a maximum coolant temperature of 3000 R (resulting from an assumed maximum temperature of the BeO portion of 3000 R) and at a value of X of 0.33 ft (10 cm) for a maximum coolant temperature of 5000 R. The D_2O portions of a graphite-D_2O moderator may be initiated at values of X of 1.03 and 0.71 ft (32 and 22 cm) for maximum coolant temperatures of 5000 and 3000 R, respectively. The minimum values of X for which D_2O may be used are also lower when a BeO layer is employed inside of the D_2O layer. It can be seen from Fig. 11 that the use of a composite moderator should permit heavy water to be employed in a large fraction of the moderator volume.

Partial Cooling Using Auxiliary Coolant Loop

Two problems which are inherent in the cycle shown in Fig. 8a can be overcome by use of the cycle shown in Fig. 8b. In Fig. 8b it is assumed that the heat deposited in the outer portion of the moderator-reflector is removed by an auxiliary coolant loop which is then used to transfer the heat to the pump exit flow using the counterflow heat exchanger shown in this figure. The power for the pump required in the auxiliary coolant loop would be obtained from the turbine in the propellant circuit. According to an approximate analysis in Appendix IV, the weight associated with the tubes in this counterflow heat exchanger would be approximately 17,000 lb if steel having a wall thickness of 0.010 in. can be employed in this heat exchanger.

The most important advantage which will result from use of the auxiliary coolant loop shown in Fig. 8b is that most of the pressure drop within the moderator-reflector resulting from the use of the cycle shown in Fig. 8a (see Fig. 10) can be eliminated. If the coolant cycle shown in Fig. 8a is employed, it may be impossible to support the moderator structure without the use of nonmoderator materials which might have a substantial adverse effect on required critical mass. In the configuration shown in Fig. 8b, the pressure in the auxiliary coolant loop would be adjusted so as to minimize the radial pressure gradient in the moderator, thereby causing a high pressure difference across the walls of the tubes in the counterflow heat exchanger. However, a high pressure difference in this heat exchanger can probably be tolerated because of the greater choice of materials available when neutron absorption and moderating characteristics are not important. For instance, an allowable wall stress of 20,000 psi in a tube having a wall thickness of 0.010 in. and a diameter of 0.1 in. would permit a pressure difference across the tube wall of 4000 psi or 270 atm.

A second advantage of the cooling cycle shown in Fig. 8b is that it may be used to eliminate the presence of the hydrogen propellant in a portion of the moderator region. The presence of hydrogen coolant in a moderator is undesirable because of the large absorption cross section of hydrogen relative to any of the other conventional moderator materials. For instance, according to Ref. 14 it is impossible to attain criticality in a thermal-neutron cavity reactor for any fuel density or any reactor size if light water is employed as a moderator-reflector. The effect of the presence of hydrogen coolant on macroscopic moderator absorption coefficient is shown in Fig. 12 for a graphite moderator. The curves for zero hydrogen pressure indicate the absorption characteristics of the graphite moderator employed. It can be seen that filling the coolant passages with high-pressure hydrogen results in substantial increases in macroscopic absorption cross section. For instance, for a temperature of 1000 R, a hydrogen pressure of 1000 atm, and a coolant passage volume of 1/10 of the total volume, the macroscopic absorption cross section is increased by a factor of almost four. The fractional increase in absorption coefficient would be even greater if hydrogen coolant were used to cool a heavy-water moderator because of the low inherent absorption coefficient of pure heavy water. Therefore, in the configuration shown in Fig. 8b, it would be desirable to employ as the coolant fluid helium, liquid heavy water, gaseous heavy water, or gaseous deuterium. Such a design would substantially reduce neutron absorption in all parts of the moderator influenced by this auxiliary coolant loop.

Full Cooling Using Auxiliary Coolant Loop

Advantages may be gained by removing all of the heat deposited in the moderator by an auxiliary coolant loop as shown in Fig. 8c rather than a portion of this heat deposition as indicated by Fig. 8b. Such a configuration could employ a "low-temperature" heat exchanger to transfer heat to the pump-exit flow, but would require a "high-temperature" heat exchanger to transfer heat to the turbine exit flow and raise the temperature of the propellant from the turbine exit temperature (on the order of 2000 R) to the desired cavity injection temperature (on the order of 5000 R). This high-temperature heat exchanger could be made out of materials such as graphite, tungsten, tantalum, or hafnium without regard to the neutron absorption characteristics of these materials. Although the absolute temperature in this portion of the counterflow heat exchanger would be high, the pressure difference across the walls of this portion of the heat exchanger would be much less than that across the low-temperature heat exchanger used to transfer energy to the pump-exit flow. If wall material thicknesses on the order of 0.010 in. were allowable in the high-temperature heat exchanger, the weight of the tubes in this heat exchanger would be of the same order as the 17,000 lb estimated for the low-temperature heat exchanger in Appendix IV.

The first advantage to be gained by using a full auxiliary coolant loop rather than a partial auxiliary coolant loop is that hydrogen would be removed from an additional portion of the moderator. Although the volume occupied by the high-temperature portion of the moderator is less than that occupied by the low-temperature

portion of the moderator (see Fig. 10), and the macroscopic absorption cross section is less (see Fig. 12), the neutron flux and hence the tendency to absorb neutrons is greater near the surface of the cavity than near the outside portion of the moderator.

The second advantage resulting from the use of the configuration shown in Fig. 8c is that the problem of hydrogen attack on graphite at high temperatures would be eliminated from the moderator. According to Ref. 15, graphite reacts with hydrogen at temperatures greater than approximately 2800 F (3260 R). The use of helium as a fluid in the auxiliary coolant loop would result in minimizing chemical attack on the moderator material.

Cycle with Outward Coolant Flow

Duct configurations which will permit cooling of the moderator-reflector by passage of the coolant fluid from the inside to the outside of the moderator are shown in Fig. 13. The straight and wavy duct passages shown in Fig. 13 have the same significance as in Fig. 8. One reason for the outward flow of coolant fluid is to provide the lowest temperatures near the inside edge of the moderator in order to reduce the temperature of the neutrons in the fuel-containment region. This is desirable since a decrease in neutron temperature will usually result in a decrease in the fuel density required for criticality.

Temperature distributions determined for outward coolant passage flow are shown in Fig. 14 for maximum coolant temperatures of 3000 and 5000 R. The temperature rise in each segment was made proportional to the heat deposition rate shown in Fig. 4 in a manner similar to that described in a preceding section. It can be seen from Fig. 14 that it is possible to employ heavy water near the inside surface of the moderator for distances up to 0.15 and 0.26 ft (4.6 and 8.0 cm) for maximum coolant temperatures of 5000 and 3000 R, respectively. Such configurations may be superior to those indicated in Fig. 11 because of the reduction in neutron temperature in the fuel region and because the heavy-water portion of the moderator is located close to the fuel region where its superior neutron moderating and absorption properties have the greatest effect. However, the fraction of the moderator which may be heavy water is much less for the temperature distributions in Fig. 14 than for the temperature distributions in Fig. 11. Detailed analyses are required to determine which of these configurations will result in the lowest critical fuel mass.

Calculations in a preceding section indicate that the temperature on the inside surface of the moderator would be required to have a value approximately equal to the gas temperature immediately within the cavity in order to minimize convective heat transfer from the cavity to the wall. Under these conditions, a relatively small amount of heat flow from this inside surface to the coolant duct nearest to the surface would be required to provide a substantial temperature gradient in the moderator in this region. The extent of the region of high temperature between the innermost coolant duct and the interface between the moderator and cavity would be

very small relative to a neutron mean-free-path in the moderator and would have a very small influence on the temperature of the neutrons passing through this portion of the moderator.

Cycle with Combined Inward and Outward Coolant Flow

The coolant duct configurations shown in Fig. 15 would permit cooling of the outer portion of the moderator by inward coolant flow and the inner portion of the moderator by outward coolant flow. The use of such coolant duct configurations would permit attainment of coolant temperature distributions such as those shown in Fig. 16. According to Fig. 16, the heavy-water portion of the moderator occupies a large fraction of the outer volume of the moderator (at distances greater than 0.88 and 0.36 ft (27 and 11 cm) for maximum coolant temperatures of 5000 and 3000 R, respectively). Thus the fraction of moderator volume which may be made up of heavy water is almost as great as that shown in Fig. 11. In addition, the outward coolant flow near the inside portion of the moderator permits use of a relatively cold moderator in this region and gives rise to relatively cold neutron temperatures in the fuel-containment region. Although these neutron temperatures are not as low as those which would result from the coolant temperature distributions shown in Fig. 14, they are substantially lower than the neutron temperature distribution which would result from the coolant temperature distributions shown in Fig. 11. Thus the coolant configurations shown in Fig. 15 retain a major portion of the advantages to be gained from the configurations shown in both Figs. 8 and 13. It is also possible to limit the maximum temperatures in the heavy-water region to somewhat less than 1000 R, thereby reducing the fraction of the moderator volume devoted to heavy water, but at the same time causing a greater reduction in neutron temperature. Detailed analyses of the criticality requirements of each of these configurations are required to determine the configuration which will result in the lowest required critical mass.

DETAILS OF COOLANT FLOW CHARACTERISTICS

Coolant Flow Within Moderator Interior

Heat Conduction Within Moderator Wall

The geometry of the coolant passages within the moderator wall must be chosen to provide an acceptable temperature difference between the point within the wall furthest from the coolant passages and points located on the surface of the coolant passages. Estimates of this temperature difference for a triangular array of coolant passages were obtained from the results of the analysis of Ref. 16 for values of coolant passage volume fraction, V_P , greater than 0.06. For values of V_P less than 0.06, the results of Ref. 16 were extrapolated using as a guide the results of an analysis of the temperature distribution in a uniformly-heated circular cylinder

with heat removal through a duct located on the centerline of the cylinder. In the following discussion it is either assumed that the temperature gradient illustrated in Fig. 10 is small compared to the temperature gradient required to conduct heat to the coolant passages or it is assumed that the resulting temperature distributions can be combined. It can be shown from Ref. 16 that:

$$T_{W_M} - T_W = \frac{Q_V}{k_m} d^2 f(V_P) \tag{2}$$

In evaluating Eq. (2), the following value of graphite conductivity from Table 42-II of Ref. 15 was employed:

$$k_m = 140 \frac{\text{BTU}}{\text{HR-FT}^2\left(\frac{^\circ\text{R}}{\text{IN.}}\right)} = 3.24 \times 10^{-3} \frac{\text{BTU}}{\text{SEC-FT}^2\left(\frac{^\circ\text{R}}{\text{FT}}\right)} \tag{3}$$

The results of evaluating Eq. (2) using a heat deposition rate per unit volume, Q_V, of 10^5 BTU/sec-ft^3 are given by the curves which are read from the ordinate on the left side of Fig. 17. It can be seen from this figure that small values of V_P and large values of coolant passage diameter lead to extremely high indicated values of temperature difference. However, large values of V_P and small values of coolant passage diameter lead to relatively small values of this temperature difference. The permissible heat deposition rate is also shown in Fig. 17 as a function of V_P for an assumed permissible value of $T_{W_M}-T_W$ of 500 R.

Because of the large number of variables which are considered in the analysis of coolant duct geometries, a nominal design point has been selected in order to provide a reference for choosing representative numbers from each theoretical curve. This nominal design is assumed to employ coolant passages having diameters of 0.02 in. and a coolant passage volume fraction of 0.05. It is also assumed that the heat deposition rate is 10^5 BTU/sec-ft^3 (approximately equal to that of the reference engine of Fig. 2). For the design point, the temperature difference plotted in Fig. 17 is approximately 230 R.

Curves which permit calculation of the surface area of the internal walls of the coolant passages are given in Fig. 18. This information is of use because under some conditions it is necessary to protect the walls of the coolant passages from chemical attack by the propellant. It can be seen from Fig. 18 that the coolant passage surface area is approximately 120 times the surface area of the internal cavity for each foot of moderator depth for the nominal design point. According to Table 42-II of Ref. 15, graphite is subject to hydrogen attack at temperatures above approximately 3260 R. Also, according to Fig. 10, the moderator temperature is above 3260 R for distances less than approximately 0.3 ft from the internal wall of the moderator. Therefore, the internal tube surface area which would have to be protected from hydrogen attack would be approximately 36 times the internal surface area of the moderator cavity for the nominal design point.

The effect of coolant passage volume fraction on the number of coolant passages per unit surface area is shown in Fig. 19. It will be shown in a following subsection that the required slope of the coolant passages, $\Delta\ell/\Delta X$, for the nominal design point is approximately 2.9. (The term "slope" is used although $\Delta\ell/\Delta X$ is actually equal to the cosecant of the angle between the passage centerline and the cavity surface.) For this condition, approximately 8100 coolant passages would be required per square foot of moderator surface area or approximately 56 coolant passages per square inch of moderator surface area.

Heat Transfer from Coolant Passage Wall to Propellant

Differential Relations

The heat removed from the wall of the coolant passages in depth ΔX per unit area A_S due to the difference between the temperature of the coolant passage wall and the average local temperature of the propellant is given by the following conventional equation involving the film coefficient:

$$\Delta Q = h \frac{\Delta A_W}{A_S} (T_W - T_C) \tag{4}$$

The internal surface area of the coolant passage walls in the preceding expression is:

$$\Delta A_W = A_S N \pi d \Delta \ell \tag{5}$$

According to p. 168 of Ref. 17, the film coefficient is given by the following equation:

$$h = 0.023 \frac{k}{d} Re_d^{0.8} Pr^{1/3} \tag{6}$$

The definition of heat deposition rate per unit volume is as follows:

$$Q_V = \frac{\Delta Q}{\Delta X} \tag{7}$$

Equations (4) through (7) have been combined using the expressions which define the coolant passage volume fraction, V_P, and the number of tubes per unit surface area, N, to yield the following expression for Reynolds number within the coolant passages.

$$Re_d = \frac{d^{2.5}\, Pr^{5/6}}{0.0507} \left(\frac{Q_V}{V_P C_P \mu (T_W - T_C)} \right)^{1.25} \tag{8}$$

Equation (8) has been evaluated and plotted in Fig. 20 using the following values of hydrogen properties determined for a representative gas temperature of 4000 R:

$$C_P = 4.2 \text{ BTU/LB } ^\circ R \tag{9}$$

$$\mu = 2.24 \times 10^{-5} \text{ LB/SEC-FT} \tag{10}$$

$$Pr = 0.65 \tag{11}$$

$$k = 14.5 \times 10^{-5} \text{ BTU/SEC-FT-}^\circ R \tag{12}$$

For the nominal design point, the Reynolds number is approximately 16,000. Maximum values of Q_V for a temperature difference, $T_{W_M} - T_W$, of 500 deg (see Fig. 17) are noted in Fig. 20 by circular symbols. The cross symbols in Fig. 20 are used to denote a Reynolds number of 5000 which is the approximate minimum Reynolds number for which Eq. (6) is valid (i.e., the approximate minimum Reynolds number for turbulent flow).

The heat which is transferred from the coolant passage wall to the propellant is related to the propellant flow as follows:

$$\Delta Q = W C_P \Delta T_C \tag{13}$$

where

$$W = \rho V \frac{\pi}{4} d^2 N \tag{14}$$

The following expression for the slope of the coolant passages can be obtained by combining Eqs. (7), (8), (13), (14), and the definition of Reynolds number:

$$\frac{\Delta \ell}{\Delta X} = \frac{d^{1.5} Pr^{5/6}}{0.0507 (T_W - T_C)^{1.25}} \frac{\Delta T_C}{\Delta X} \left(\frac{Q_V}{V_P C_P \mu} \right)^{0.25} \tag{15}$$

The slope of the coolant passages as determined from Eq. (15) is plotted in Fig. 21 for the same conditions employed in Fig. 20. In addition, a value of $\Delta T_C/\Delta X$ of 6000 R/ft was selected on the basis of the results shown in Fig. 10. It can be seen from Fig. 21 that the required coolant passage slope is approximately 2.9 for the nominal design point noted in preceding paragraphs. Both the Reynolds number and the slope of the coolant passages are independent of the pressure level of the propellant.

The velocity within the coolant passages may be determined from the definition of Reynolds number and from Eq. (8) as follows:

$$V = \frac{d^{1.5} Pr^{5/6}}{0.0507 \rho \mu^{0.25}} \left(\frac{Q_V}{V_P C_P (T_W - T_C)} \right)^{1.25} \tag{16}$$

Equation (16) is plotted in Fig. 22. It can be seen from Fig. 22 that the velocity in the coolant passage is approximately 320 ft/sec for the nominal design point noted in preceding paragraphs.

The dynamic pressure of the flow in the coolant passages can be obtained from the velocity given by Eq. (16).

$$q = \frac{1}{0.00514 g \rho} \frac{d^3 Pr^{5/3}}{\mu^{0.5}} \left(\frac{Q_V}{V_P C_P (T_W - T_C)} \right)^{2.5} \tag{17}$$

Values of dynamic pressure determined from Eq. (17) are given in Fig. 23. It can be seen from Fig. 23 that the dynamic pressure is approximately 0.57 atm for the nominal design point discussed in preceding paragraphs.

According to p. 127 of Ref. 17,

$$\Delta P = 4fq \frac{\Delta \ell}{d} \tag{18}$$

Also, according to p. 119 of Ref. 17, for turbulent flow in smooth pipes,

$$f = \frac{0.046}{Re_d^{0.2}} \tag{19}$$

Combining Eqs. (15), (17), (18), and (19) yields

$$\frac{\Delta P}{\Delta X} = \frac{d^3 Pr^{7/3}}{0.00257\ g\ \rho\ \mu^{0.50}(T_W - T_C)^{3.5}} \frac{\Delta T_C}{\Delta X} \left(\frac{Q_V}{V_P C_P}\right)^{2.5} \tag{20}$$

Equation (20) is plotted in Fig. 24 for the same conditions noted in Figs. 20 through 23. It can be seen from Fig. 24 that the pressure gradient normal to the wall is approximately 25 atm/ft for the nominal design point noted in preceding paragraphs. Figs. 22, 23, and 24 were obtained on the basis of a hydrogen pressure of 1000 atm (density at a temperature of 4000 R of 0.69 lb/ft^3). It can be seen from Eqs. (16), (17), and (20) that velocity, dynamic pressure, and pressure gradient are all inversely proportional to density (or pressure at a given value of temperature). Therefore, the quantities given in Figs. 22, 23, and 24 are inversely proportional to pressure for values of pressure other than 1000 atm.

The moderator pressure gradient for a value of Q_V of 10^5 $BTU/sec\text{-}ft^3$ is given in Fig. 25 as a function of coolant passage volume fraction for three different coolant passage diameters and for three different values of temperature difference between the coolant passage wall and the propellant.

As noted on Figs. 20 through 25, all calculations were made on the basis of a gas temperature, T_C, of 4000 R. The effect of changes in this gas temperature on pressure gradient can be determined from Eq. (20). Assume that the following are fixed: d, V_P, Q_V, $T_W - T_C$, Pr, and C_P. If the attenuation constant for energy deposition by neutrons and gamma rays is also fixed (see Fig. 3),

$$\frac{\Delta T_C}{\Delta X} \sim T_C \tag{21}$$

Also assume that:

$$\rho \sim \frac{1}{T_c}$$
$$\mu \sim T_c^{0.75} \tag{22}$$

If Eqs. (21) and (22) are substituted in Eq. (20), it can be shown that

$$\frac{\Delta P}{\Delta x} \sim T_c^{1.625} \tag{23}$$

Thus, if the nominal design point had been evaluated for a temperature of 6000 R rather than a temperature of 4000 R, the pressure gradients would have been 1.93 times the pressure gradients indicated in Figs. 24 and 25.

Integrated Results

It is now of interest to integrate the expression for pressure gradient given by Eq. (20) to determine the pressure drop through a given portion of the moderator-reflector for the case of inward coolant flow (see Figs. 8, 10, and 11). It is assumed that the following are constant in performing this integration: d, N, $T_w - T_c$, C_p, and Pr. It is also assumed that the heat deposition rate, Q_v, falls off logarithmically with the distance from the surface of the moderator (see Fig. 3).

$$\frac{Q_v}{Q_{v_1}} = \frac{1}{e^{\alpha x}} \tag{24}$$

The local heat deposition rate must be equal to the rate at which heat is carried away by the coolant. If the coolant flow rate and specific heat are constant, if discontinuities in temperature such as those due to the turbopump cycle (see Fig. 10) are neglected, and if $T_c = 0$ when heat flux is zero, then

$$\frac{T_c}{T_{c_1}} = \frac{1}{e^{\alpha x}} \tag{25}$$

and

$$\frac{\Delta T_c/\Delta x}{(\Delta T_c/\Delta x)_1} = \frac{1}{e^{\alpha x}} \tag{26}$$

A sketch showing the variation of heat deposition rate and temperature with distance through the moderator according to these assumptions is given on the top of Fig. 26. Also assume that

$$\frac{\rho}{\rho_1} = \frac{T_{C_1}}{T_C} = e^{\alpha X} \tag{27}$$

$$\frac{\mu}{\mu_1} = \left(\frac{T_C}{T_{C_1}}\right)^{0.75} = \frac{1}{e^{0.75\alpha X}} \tag{28}$$

If Eqs. (24) through (28) are substituted in Eq. (15), it can be shown that

$$\frac{\Delta \ell / \Delta X}{(\Delta \ell / \Delta X)_1} = \frac{V_P}{V_{P_1}} = \frac{1}{e^{0.85\alpha X}} \tag{29}$$

Since the slope of the coolant passage, $\Delta \ell / \Delta X$, must be greater than unity, the assumptions employed to develop the preceding equations are valid only for a limited distance into the moderator. If, for example, $(\Delta \ell / \Delta X)_1$, is assumed to be 2.9 (the value for the nominal design condition), the limiting dimensionless distance αX for which the analysis is valid is 1.25. However, at this point both the heat deposition rate and the temperature have fallen to approximately 29 percent of their values at Station 1.

Substitution of Eqs. (24) through (29) in Eq. (20) yields

$$\frac{\Delta P / \Delta X}{(\Delta P / \Delta X)_1} = \frac{1}{e^{2\alpha X}} \tag{30}$$

This equation may be integrated to obtain

$$P - P_1 = \frac{(dP/dX)_1}{2\alpha} \left(1 - \frac{1}{e^{2\alpha X}}\right) \tag{31}$$

The preceding equation is plotted in the lower portion of Fig. 26. If the attenuation parameter α is assumed to be 1.5 ft^{-1}, the pressure drop through the moderator is always less than one-third of the pressure gradient (measured in atm/ft) such as the values of pressure gradient plotted in Figs. 24 and 25. Therefore, the pressure drop for the nominal design point discussed in preceding sections is approximately 8 atm. Values of pressure drop of this order of magnitude can be obtained for

heat deposition rates considerably greater than 10^5 BTU/sec-ft^3 if the coolant passage volume fraction is increased or if the coolant passage diameter is decreased from the nominal design values. A detailed structural analysis is required to determine the permissible pressure drop within the moderator.

Effect of Change of Coolant Fluid

Although hydrogen is the moderator coolant fluid normally considered in gaseous nuclear rockets, it may be desirable to employ alternative coolant fluids such as deuterium, water, heavy water, helium, methane, and ammonia for reasons which are discussed in Appendix II and in the section entitled MODERATOR COOLANT FLOW CYCLES. Substitution of an alternative coolant for hydrogen changes only the heat transfer characteristics within the coolant passage, and has no effect on heat conduction within the moderator wall (see Figs. 17 through 19). The heat transfer from the coolant passage wall to the propellant is governed by the properties of the coolant fluid, the heat deposition rate per unit volume, Q_V, the diameter of the coolant passage, d, the temperature difference between the wall and the coolant, $T_W - T_C$, and the coolant passage volume fraction, V_P.

Results from Ref. 12 of studies of the properties of various coolant fluids are given in Table III. Note that the properties for hydrogen are slightly different than those given by Eqs. (9) through (12) and which are noted as the reference properties of hydrogen. The ratio of the density, specific heat, viscosity, and Prandtl number for each of the coolant fluids to the corresponding reference values for hydrogen are also shown in Table III. It should be noted that all data shown are for the pure gas with no correction for any dissociation which may occur at the temperature and pressure considered.

The Reynolds number of the flow within the moderator coolant passages is given by Eq. (8) in the preceding section. It can be seen by examination of Eq. (8) that a change in fluid properties for fixed values of Q_V, d, V_P, and $T_W - T_C$ would result in the following effect on Reynolds number:

$$\frac{Re_d}{(Re_d)_{REF}} = \left(\frac{Pr}{Pr_{REF}}\right)^{5/6} \left(\frac{(C_P \mu)_{REF}}{C_P \mu}\right)^{1.25} \qquad (32)$$

The results of evaluating Eq. (32) using the ratios of fluid properties from Table III are given in the second column of Table IV. It can be seen from Table IV that the Reynolds number for coolant fluids other than hydrogen are greater than those for hydrogen. The factors noted in this table can be employed with the Reynolds numbers noted in Fig. 20 to determine absolute Reynolds numbers for a wide variety of conditions.

The procedure employed to determine the effect of changes in coolant fluid on passage Reynolds number were also employed to determine the effect of changes in coolant fluid on the slope of the coolant passages, $\Delta \ell / \Delta X$, the velocity in the

coolant passages, V , the dynamic pressure in the coolant passages, q , and the pressure gradient within the coolant passages, $\Delta P/\Delta X$. These relations were obtained from Eqs. (15), (16), (17), and (20) and are given in the last four columns of Table IV. Absolute values of these quantities can be obtained by applying the corrections shown in Table IV to the curves shown in Figs. 21 through 25.

Since the pressure drop across any portion of the moderator is related to the pressure gradient within these passages, the pressure gradient ratios shown in the last column of Table IV also indicate the difference in pressure drop when alternative coolant fluids are substituted for hydrogen. Although the pressure gradient and, hence, the pressure drop are greater when alternative coolant fluids are employed, it may be possible to change the geometry of the coolant passages in order to minimize the change in pressure drop resulting from the use of alternative coolant fluids. For instance, if helium were employed rather than hydrogen, the tendency to neutron poisoning in the moderator and the tendency toward chemical attack on the moderator walls would be reduced. Therefore, it would be possible to employ much larger coolant passage volume fractions and smaller coolant passage diameters using helium as a coolant fluid than those which would be chosen using hydrogen as a coolant fluid. According to Eq. (20), either a reduction in coolant passage diameter or an increase in coolant passage volume fraction would result in a substantial reduction in coolant passage pressure gradient normal to the wall, thereby compensating for the change in properties between these coolant fluids.

As noted in a preceding paragraph, the data in Table III and, hence, the data in Table IV, were determined on the basis of no dissociation of the coolant fluids. According to Ref. 12, this assumption is valid for all of the coolant fluids shown except methane. At 4000 R, methane undergoes considerable dissociation which results in the formation of substantial factions of solid graphite. This formation of solid graphite, and the resulting tendency to clog coolant ducts, could be avoided by using a mixture of carbon to hydrogen with a weight ratio of 0.73. The resulting mixture would have properties midway between those for hydrogen and those for methane shown in Tables III and IV. Use of such a mixture would eliminate the tendency for propellant attack on graphite at 4500 R, but would not eliminate this tendency for temperatures less than and greater than 4500 R. The relative values of properties for methane and hydrogen shown in Tables III and IV are valid for temperatures below 2000 R where the dissociation of methane is small.

Coolant Flow Near Moderator Surface

The heat flux which can be conducted away from the inside surface of the moderator wall is proportional to the difference between the cavity wall temperature, T_{w_c} , and the temperature of the wall of the coolant duct, T_w (see Fig. 6). Thus

$$\left(\frac{Q}{A}\right)_{CONDUCTION} = -k_m \frac{T_{W_C} - T_W}{X_W} \qquad (33)$$

In the calculations discussed in the following paragraphs it is assumed that the internal conductivity of the wall material is given by Eq. (3). The effective thickness of the coolant passage wall (X_W in Eq. (33)) may be made to be very small if some form of transpiration cooling is employed (i.e., if the average distance from the moderator surface to the nearest pore of the porous wall is extremely small). However, in some forms of gaseous nuclear rocket engines it is desirable to inject the fluid coming into the cavity with a velocity which is much greater than that obtainable through the pores associated with transpiration cooling. Therefore, if transpiration cooling is not employed, the heat flux may be limited by the minimum permissible thickness of the structural wall. For the following calculations it is assumed that the minimum thickness of the wall is 0.002 ft (approximately 0.02 in.).

If the moderator cooling fluid passes radially inward through the moderator structure (such as indicated in Fig. 8), it is desirable to minimize the temperature difference between the wall and the cooling fluid in order to maximize the temperature of the propellant injected into the cavity. If the corresponding temperature difference in thickness X_W is assumed to be 200 R, then the maximum heat transfer per unit area according to Eq. (33) is equal to:

$$\left(\frac{Q}{A}\right)_{CONDUCTION} = 3.24 \times 10^{-3} \left(\frac{200}{0.002}\right) = 324 \frac{BTU}{SEC-FT^2} \qquad (34)$$

This heat flux is equal to less than 0.5 percent of the heat flow normal to the wall due to neutrons and gamma rays. The neutron and gamma ray energy deposited in a thickness of 0.002 ft would be approximately 230 BTU/sec-ft^2. Therefore, the total temperature difference across this thickness of 0.002 ft would have to be somewhat greater than 200 R to permit transfer to the wall of the coolant tube of both the heat deposited on the internal surface of the cavity (see Table II) and the heat deposited immediately inside of the surface. The velocities in the coolant tube or the temperature difference between the coolant tube wall and the coolant fluid would have to be increased relative to the values which were calculated for neutron and gamma heating alone to obtain the additional heat transfer capacity required to remove the heat deposited on the internal cavity surface.

The heat transfer rate from the internal cavity wall by conduction given by Eq. (34) may be smaller than the heat deposition rate on the surface of the moderator from various sources (see Table II). In such instances, it may be necessary to obtain increased cooling by establishing a larger temperature difference. This can be accomplished by ducting the coolant fluid to the portion of the moderator near the

cavity surface before it is employed to cool the remaining portion of the moderator structure (see Figs. 13 and 15). In such an instance it might be possible to employ a temperature difference of 2000 R in a distance equal to the thickness X_W. Under such circumstances, the heat removal rate according to Eq. (33) would be:

$$\left(\frac{Q}{A}\right)_{CONDUCTION} = 3.24 \times 10^{-3}\left(\frac{2000}{0.002}\right) = 3240 \frac{BTU}{SEC-FT^2} \qquad (35)$$

Such a heat removal rate by conduction is probably sufficient to cause removal of the heat deposited on the internal cavity surface if a magnetic field is employed to reduce beta particle heating (see Table II). An increase in coolant velocity or temperature difference between the moderator wall and the coolant fluid would be required to cause transfer of this energy to the coolant fluid. As noted in a preceding paragraph, if the heat transfer rate by conduction given by Eq. (35) is insufficient to provide acceptable wall cooling, the only remaining solution is to effectively reduce the distance over which the heat must be conducted, possibly by the employment of transpiration cooling.

REFERENCES

1. Weinstein, H., and R. Ragsdale: A Coaxial Flow Reactor -- A Gaseous Nuclear-Rocket Concept. ARS Preprint 1518-60, presented at the ARS 15th Annual Meeting, Washington, D. C., December 1960.

2. Kerrebrock, J., and R. Meghreblian: An Analysis of Vortex Tubes for Combined Gas-Phase Fission-Heating and Separation of the Fissionable Material. ORNL CF 57-11-3, Revision 1, April 11, 1958.

3. Paul, D. J.: Effect of Fission Product Residence Time on Fraction of Fission Energy Deposited in Walls of a Gaseous Nuclear Rocket. UAC Research Laboratories Report UAR-B139, September 4, 1963.

4. Bussard, R. W., and R. D. DeLauer: Nuclear Rocket Propulsion. McGraw-Hill Book Company, Inc., New York, 1958.

5. Latham, Thomas S.: Gamma and Fast Neutron Heating in Reflector-Moderators of Cavity Reactors. UAC Research Laboratories Report UAR-C27, February 24, 1964.

6. Krascella, N. L.: Theoretical Investigation of Spectral Opacities of Hydrogen and Nuclear Fuel. Report RTD-TDR-63-1101 prepared by UAC Research Laboratories, November 1963.

7. Krascella, N. L.: Tables of the Composition, Opacity, and Thermodynamic Properties of Hydrogen at High Temperatures. UAC Research Laboratories Report B-910168-1, September 1963 (Also issued as NASA SP-3005).

8. Krascella, N. L.: Theoretical Investigation of the Absorption and Scattering Characteristics of Small Particles. UAC Research Laboratories Report C-910092-1, September 1964. NASA CR-210.

9. Lanzo, Chester D., and Robert G. Ragsdale: Experimental Determination of Spectral and Total Transmissivities of Clouds of Small Particles. NASA Technical Note D-1405, September 1962.

10. Lanzo, Chester D., and Robert G. Ragsdale: Heat Transfer to a Seeded Flowing Gas From an Arc Enclosed by a Quartz Tube. NASA Technical Memorandum X-52005, Heat Transfer and Fluid Mechanics Institute, June 10 - 12, 1964.

11. Marteney, P. J.: Experimental Investigation of the Opacity of Small Particles. UAC Research Laboratories Report C-910092-2, September 1964. NASA CR-211.

12. Roback, R.: Thermodynamic Properties of Coolant Fluids and Particle Seeds for Gaseous Nuclear Rockets. UAC Research Laboratories Report C-910092-3, September 1964. NASA CR-212.

13. Davison, W. R.: Performance Analysis of Turbopump Cycles for High-Pressure Nuclear Rocket Engines. UAC Research Laboratories Report B-110056-1, July 5, 1963.

14. Safonov, G.: Externally Moderated Reactors. Rand Corporation Report R-316, July 1957.

15. Rom, Frank E., and Robert G. Ragsdale: Advanced Concepts for Nuclear Rocket Propulsion. Nuclear Rocket Propulsion, NASA SP-20, December 1962, pp. 3 - 15.

16. Sparrow, E. M.: Temperature Distribution and Heat-Transfer Results for an Internally Cooled, Heat-Generating Solid. Journal of Heat Transfer, November 1960, pp. 389 to 393.

17. McAdams, William H.: Heat Transmission. McGraw-Hill Book Company, Inc., New York, 1942.

18. Shepherd, L. R., and A. V. Cleaver: The Atomic Rocket--3. J. Brit., Interplanet. Soc., Vol. 8, No. 1, pp. 23 - 24, 30 - 37, January 1949.

19. Arnoldi, R.: A Method of Calculating Size and Composition of Gaseous Nuclear Rocket Reactors. UAC Research Laboratories Report M-1686-4, April 1960.

20. Hunter, Maxwell W., Jr.: The Potential for Nuclear Propulsion for Manned Spaceflights. Presented at the National Meeting on Manned Space Flight, Institute of the Aerospace Sciences, St. Louis, Missouri, April 20 - May 2, 1962.

21. Meghreblian, Robert V.: Performance Potential of Nuclear Rockets. CIT/JPL Report TR 34-96, July 1960.

LIST OF SYMBOLS

a_e	Extinction coefficient for thermal radiation, cm^{-1}
A_S	Surface area of internal wall of moderator-reflector, ft^2
ΔA_W	Surface area of coolant passages in wall thickness ΔX, ft^2
b_e	Particle extinction parameter, cm^2/gm
C_N	Ratio of thrust to thrust calculated assuming complete conversion of thermal energy to velocity energy
C_P	Specific heat of coolant, BTU/lb-deg R
d	Diameter of coolant passage, in. or ft
f	Friction factor (see Eq. (19))
g	Acceleration due to gravity, 32.2 ft/sec^2
h	Film coefficient (see Eqs. (4) and (6)), BTU/sec-ft^2-deg R
H	Enthalpy, BTU/lb
H_{EXIT}	Enthalpy of gases passing through nozzle of gaseous nuclear rocket, BTU/lb
H_W	Enthalpy of gases injected into reaction chamber of gaseous nuclear rocket, BTU/lb
I	Thermal radiation passing through seeded hydrogen layer, BTU/sec-ft^2
I_O	Thermal radiation incident on seeded hydrogen layer, BTU/sec-ft^2
I_{SP}	Specific impulse, sec
k	Thermal conductivity of coolant, BTU/sec-ft^2-(deg R/ft)
k_m	Thermal conductivity of moderator, BTU/hr-ft^2-(deg R/in.) or BTU/sec-ft^2-(deg R/ft)
ℓ	Length of nozzle passages (see Fig. 18), in.

N	Number of coolant passages divided by surface area A_S, ft^{-2}
P	Pressure, atm
ΔP	Pressure drop of coolant in thickness ΔX, lb/ft^2 or atm
P_H	Hydrogen pressure, atm
Pr	Prandtl number, $C_P \mu / k$
q	Dynamic pressure of propellant in coolant passages, lb/ft^2 or atm
ΔQ	Heat deposition in moderator in thickness ΔX per unit area, A_S, $BTU/sec\text{-}ft^2$
$\left(\frac{Q}{A}\right)_{CONDUCTION}$	Heat flux through wall of inside surface of cavity due to thermal conduction (see Eq. (33)), $BTU/sec\text{-}ft^2$
$\left(\frac{Q}{A}\right)_{CONVECTION}$	Heat flux convected to wall from gases within cavity, (see Eq. (1)), $BTU/sec\text{-}ft^2$
Q_V	Heat deposition rate in moderator-reflector, $BTU/sec\text{-}ft^3$
r	Radial distance from engine centerline, ft
Re_d	Reynolds number based on diameter of coolant passage, $\rho V d / \mu$
St	Stanton number (see Eq. (1))
T	Temperature, deg R
T_C	Coolant temperature, deg R
T_{GAS}	Temperature of hydrogen at outside edge of boundary layer within cavity (see Fig. 6), deg R
T_W	Temperature of wall of coolant passage, deg R
T_{W_C}	Temperature of inside wall of cavity (see Fig. 6), deg R
T_{W_M}	Maximum temperature of moderator wall in region between coolant passages (see Fig. 17), deg R

V	Velocity of propellant in coolant passages, ft/sec
V_O	Hydrogen velocity at outside edge of boundary layer, ft/sec
V_P	Moderator volume fraction--volume of coolant passages divided by total moderator volume
W	Weight flow of propellant divided by moderator area A_S, lb/sec-ft^2
W_F	Fuel flow, lb/sec
W_H	Hydrogen flow, lb/sec
X	Distance from inside surface of cavity, ft
ΔX	Thickness of moderator wall in which heat deposition rate is approximately constant, ft
X_S	Thickness of seeded hydrogen layer, cm or in.
X_W	Distance from surface of moderator to nearest coolant passage (see Fig. 6), ft
Z	Distance along fizzler rocket (see Fig. 27), arbitrary units
α	Attenuation constant for energy deposition (see Eq. (24)), ft^{-1}
μ	Coolant viscosity, lb/sec-ft
ρ	Coolant density, lb/ft^3
$\bar{\rho}_F$	Average density of nuclear fuel, lb/ft^3
ρ_H	Hydrogen density, lb/ft^3
$\bar{\rho}_H$	Average hydrogen density in fizzler rocket, lb/ft^3
ρ_O	Density of hydrogen at outside edge of boundary layer within cavity, lb/ft^3
ρ_S	Density of seed material, lb/ft^3

Subscripts

$( )_{I}$	Inside surface of moderator-reflector
$( )_{Pe}$	Pump exit
$( )_{Pi}$	Pump inlet
$( )_{REF}$	Quantities determined from properties of hydrogen given by Eqs. (9) through (12)
$( )_{Te}$	Turbine exit
$( )_{Ti}$	Turbine inlet

APPENDIX I

CHARACTERISTICS OF FIZZLER ROCKET

One of the earliest proposed form of gaseous nuclear rocket engine is the fizzler rocket (see Refs. 4 and 18) in which the ratio of fuel density to propellant density is independent of position within the engine. A series of calculations was made to determine the fuel loss rate from such a rocket engine to provide a standard of comparison for more advanced gaseous nuclear rocket concepts.

The variation of hydrogen properties with distance in a fizzler nuclear rocket for a hydrogen pressure of 500 atm is given in Fig. 27. The calculations were made using a stepwise procedure in which the enthalpy rise per unit length was made proportional to the local hydrogen density (equivalent to assumption of constant neutron flux) using a constant interval in temperature of 1000 R and an initial temperature of 4000 R. The variations of hydrogen enthalpy and density with temperature were obtained from Ref. 7. The distance represented by the horizontal scale in Fig. 27 is proportional to the hydrogen flow rate and inversely proportional to the neutron flux within the engine.

Values of hydrogen enthalpy corresponding to values of hydrogen specific impulse of 1500 and 2500 sec are noted in the upper plot of Fig. 27. These enthalpies were determined on the basis of a nozzle thrust coefficient of 0.80 (defined as the actual thrust divided by the thrust theoretically attainable by expansion of the hydrogen through a perfect nozzle to zero static pressure) and by neglecting the effect of the presence of the nuclear fuel on specific impulse. It can be seen from the lower plot in Fig. 27 that the average hydrogen density from $Z = 0$ to any axial station is greater than the local hydrogen density. The ratio of these two densities is 1.51 and 2.06 for distances corresponding to enthalpies associated with values of specific impulse of 1500 and 2500 sec, respectively. These ratios were assumed to be independent of pressure at a given temperature for pressures of 100 and 1000 atm in performing calculations discussed in a following paragraph.

The ratio of hydrogen flow to fuel flow in a fizzler rocket is equal to the ratio of average hydrogen density to the average fuel density required for criticality. It was assumed that the average fuel density for criticality was given by the results of Ref. 19 which were calculated on the basis of plutonium fuel, a neutron temperature of 1500 K, and a homogenous beryllium oxide moderator occupying approximately 40 percent of the total reactor volume. The fuel was assumed to be uniformly distributed throughout the remaining reactor volume and the reactor was assumed to be cylindrical in shape with a length equal to its diameter. The resulting required average fuel densities in nonmoderator regions were 0.035, 0.011, and 0.003 lb/ft^3 for reactor diameters of 10, 20, and 50 ft, respectively.

Ratios of hydrogen flow to fuel flow determined from the results shown in Fig. 27 and the criticality requirements of Ref. 19 are given in Fig. 28. As noted in a preceding paragraph, the values of specific impulse noted on the curves were not corrected for the effect of the presence of the nuclear fuel. It can be seen from Fig. 28 that high values of the ratio of hydrogen flow to fuel flow can be obtained only for very large engines operating at high pressures. As noted in a preceding paragraph, these relative flow rates serve as a standard of comparison for more advanced gaseous nuclear rocket concepts.

APPENDIX II

EFFECT OF CHOICE OF PROPELLANT ON SPECIFIC IMPULSE OF GASEOUS NUCLEAR ROCKETS

The specific impulse of a rocket engine is a function of the enthalpy of the gases passing through the exhaust nozzle of the engine. In a gaseous nuclear rocket engine, approximately 10 percent of the total energy produced is deposited in the moderator walls (see Table I and corresponding discussion in text). If the propellant is employed to cool the moderator walls before it is injected into the engine cavity, then approximately 10 percent of the propellant enthalpy rise occurs within the moderator walls and the maximum exit enthalpy can be no greater than ten times the enthalpy corresponding to the maximum wall temperature.

Although hydrogen is the propellant usually considered for use in gaseous nuclear rockets, it is pointed out in Ref. 20 that alternate propellants such as water, methane, and ammonia are desirable because they are more easily stored than hydrogen. However, these alternate propellants absorb less energy at a given temperature than hydrogen, and hence provide lower specific impulse capabilities than is provided by hydrogen.

Quantitative information on the specific impulse capabilities of gaseous nuclear rockets using different propellants is presented in Table V. It was assumed in constructing Table V that the maximum permissible temperature of the propellant as it is injected into the engine cavity is 5300 R. The enthalpies which correspond to this temperature were obtained from Ref. 12 and are shown in the second column in this table. The exit enthalpy was then assumed to be ten times the enthalpy corresponding to a temperature of 5300 R. The specific impulse shown in the last column of Table V was determined from a velocity equal to 80 percent of the theoretical velocity obtainable by conversion of the energy associated with the exit enthalpy to kinetic energy ($C_N = 0.80$). It can be seen from this table that the specific impulse of gaseous nuclear rockets employing water, ammonia, and methane are lower than those employing hydrogen, but considerably higher than the values of specific impulse obtainable using solid-core nuclear rockets. Also shown in Table V is the specific impulse capability of an engine which employs a propellant which is 50 percent by weight hydrogen and 50 percent by weight water.

It has been suggested in Refs. 20 and 21 that the specific impulse limitation of gaseous nuclear rockets shown in Table V can be circumvented by the use of space radiators. Although space radiators would result in a decrease in over-all engine thrust-to-weight ratio, this decrease may be acceptable if high-temperature low-weight radiators can be developed. The effect of radiator temperature for a fixed radiator specific weight on the thrust-to-weight ratio characteristics of gaseous nuclear rocket engines is shown in Fig. 29. All configurations considered were

assumed to have the same power level within the basic engine. Therefore, the thrust-to-weight ratio of the engine employing water and having a specific impulse of 1200 sec is more than twice that of the engine employing hydrogen and having a specific impulse of 2500 sec (since power level for a given thrust is proportional to specific impulse). It can be seen from Fig. 29 that a low temperature in the space radiator results in significant decreases in engine thrust-to-weight ratio, but high values of radiator temperature result in relatively little decrease in engine thrust-to-weight ratio.

The radiator temperatures now envisioned for nuclear electric power supplies (on the order of 2000 R) have been chosen on the basis of consideration of cycle efficiency as well as radiator structural material characteristics. With regard to the requirements for shielding against meteoroid damage, it should be noted that a space radiator employed with a gaseous nuclear rocket would be required to operate for a time measured in minutes or hours whereas a space radiator employed with a nuclear electric power supply would be required to operate for months or years. For both of these reasons it is expected that the radiators employed with a gaseous nuclear rocket should be considerably lighter than those employed with a nuclear electric power supply for the same radiator power. Also, it should be noted that approximately 90 percent of the energy created in a nuclear electric power supply must be rejected in a space radiator, while a maximum of approximately 10 percent must be rejected in a gaseous nuclear rocket.

The values of specific impulse shown in Fig. 29 were calculated on the basis that the energy deposited in the wall was 10 percent of the total energy release in the fission process. Although this assumption is probably reasonably accurate for propellant temperatures corresponding to moderate values of specific impulse, it is probably an optimistic assumption for high values of specific impulse. For high values of specific impulse, the propellant temperatures will be so high that large amounts of energy will be transferred to the wall by thermal radiation. The resulting limitation on specific impulse was not considered in constructing the curves shown in Fig. 29.

APPENDIX III

FACILITY CONCEPT FOR TESTING GASEOUS NUCLEAR ROCKETS

A sketch showing the characteristics of a facility which could be employed for testing a gaseous nuclear rocket engine is given in Fig. 30. It is assumed in Fig. 30 that water from an upper pond at a temperature of approximately 70 F is mixed with the exhaust flow from the gaseous nuclear rocket to provide a mixture temperature of approximately 170 F before this mixture is carried to a lower pond. Following a test of the gaseous nuclear rocket engine, the water in the lower pond would be pumped back to the upper pond through a duct which contained a separator for removing fission products and any unburned nuclear fuel. The lower pond might or might not be covered. Calculations have indicated that all gaseous fission products would be soluble in the coolant water.

The mass and volume flow rates shown in Fig. 30 were calculated for a propellant flow of 1 lb/sec and a specific impulse of 2500 sec (this specific impulse is assumed to be attainable with all propellants using auxiliary cooling to simulate the effect of a space radiator in a flight engine). If hydrogen propellant were allowed to pass into the lower pond, the resulting large volume flow would require a large enclosed volume in the downstream pond assembly in order to prevent escape of hydrogen gas (which might contain fission products) to the atmosphere. Alternately, injection of approximately 8 lb/sec of oxygen with the hydrogen exhaust to permit stoichiometric combustion of the hydrogen would eliminate all gaseous exhaust and would simplify the construction of the lower pond.

The use of either water or ammonia as propellants would eliminate the need for oxygen injection (ammonia is extremely soluble in water) and simplify the construction of a facility employed to test gaseous nuclear rockets. The volume of gases produced from gaseous nuclear rocket tests employing methane as a propellant would be approximately equal to the volume of liquid produced. Although the methane exhaust products could be burned with oxygen to form water and CO_2, the solubility of CO_2 in water is so low as to necessitate much greater water flow than otherwise required to insure that all of the CO_2 gases would be dissolved in water. In tests using methane, it is probably more practical to make provisions for containing the volume of methane exhaust gases produced (this volume is approximately 13 percent of the volume of exhaust gases in tests using hydrogen as a propellant without oxygen injection).

The absolute quantity of coolant required for a given test is proportional to the thrust level of the engine and the duration of the test. If a water flow equal to 2000 times the propellant flow is assumed (see Fig. 30), the quantity of water required for a one-minute test of the reference engine of Fig. 2 would be 103 acre-feet.

APPENDIX IV

APPROXIMATE WEIGHT OF LOW-TEMPERATURE AUXILIARY HEAT EXCHANGER

It is shown in the text that the use of an auxiliary coolant loop (see Figs. 8, 13, and 15) in a gaseous nuclear rocket engine may be extremely desirable. Of particular importance is the low-temperature auxiliary coolant loop which would be employed to transfer heat to the propellant between the pump exit and the turbine inlet. The tubes in this heat exchanger could employ the same materials as the turbine. The power which would be transferred through this heat exchanger would be determined by the turbine inlet temperature, the maximum temperature attained by the propellant in cooling the wall, and the fraction of the total energy release which is deposited in the wall. For a turbine inlet temperature of 2200 R and a maximum propellant temperature within the moderator of 5000 R, approximately 44 percent of the energy deposited in the moderator would be required to pass through the low-temperature auxiliary heat exchanger. If the heat deposited in the moderator is 10 percent of the total heat release, the energy transfer in this heat exchanger would be 4.4 percent of the total energy released. For the reference engine of Fig. 2, the resulting power transfer in the heat exchanger would be 2.07×10^{7} BTU/sec (2.18×10^{4} megw).

The heat transfer rate through the walls of this heat exchanger is given by the following:

$$\left(\begin{array}{c}\text{Heat Flow} \\ \text{Per Unit Area}\end{array}\right) = (\text{Thermal Conductivity}) \frac{\left(\begin{array}{c}\text{Temperature Difference} \\ \text{Across Wall}\end{array}\right)}{(\text{Wall Thickness})}$$

If this relation is evaluated from the following:

$$(\text{Thermal Conductivity}) = 15 \text{ BTU/hr-ft}^2\text{-(deg R/ft)} = 4.16 \times 10^{-3} \text{ BTU/sec-ft}^2\text{-(deg R/ft)}$$

$$(\text{Temperature Difference}) = 100 \text{ R}$$

$$(\text{Wall Thickness}) = 0.010 \text{ in.} = 8.33 \times 10^{-4} \text{ ft}$$

Then,

$$(\text{Heat Flow Per Unit Area}) = 500 \text{ BTU/sec-ft}^2$$

The required area within the coolant tubes obtained by dividing the total power transferred in the heat exchanger by the heat transfer per unit area is 41,400 ft^2,

and the volume of metal in these tubes is 34.5 ft^3. If the density of this metal is assumed to be 500 lb/ft^3, the weight of the tubes in the heat exchanger would be 17,200 lb. It can be shown that this weight is proportional to the square of the wall thickness and to the reciprocal of the temperature difference across the wall.

TABLE I

ENERGY RELEASE DUE TO FISSION OF PLUTONIUM-239

Data from Ref. 3

	Absolute Energy Release, Mev/fission		Fraction of Energy Release		Absolute Energy Release, BTU/sec-ft^2, for Total Energy Release of 10^6 BTU/sec per Square Foot of Cavity Surface Area	
	5 sec After Fission	100 sec After Fission	5 sec After Fission	100 sec After Fission	5 sec After Fission	100 sec After Fission
Neutron Energy	6.0	6.0	0.032	0.031	32,000	31,000
Gamma Ray Energy	7.2	9.1	0.038	0.047	38,000	47,000
Fission Fragment Energy	172	172	0.917	0.890	917,000	890,000
Beta Particle Energy	2.5	6.1	0.013	0.032	13,000	32,000
Total	187.7	193.2	1.000	1.000	1,000,000	1,000,000

TABLE II

SUMMARY OF CALCULATIONS OF MODERATOR HEATING FOR REFERENCE ENGINE

See Fig. 2 for Description of Reference Engine

Phenomena	Source of Information	Volume Heat Deposition Rate Immediately Inside Surface of Moderator, , BTU/sec-ft^3	Surface Heating Rate, BTU/sec-ft^2
Fission Fragment Impingement	Text	--	0
Neutron and Gamma Heating	Text, Fig. 3	110,000 to 122,000	--
Beta Particle Impingement	Text	--	+6000 to +16,000 (no magnetic field) +120 to +1200 (with magnetic field)
Thermal Radiation	Text, Fig. 5	--	+200 to +2000
Convection from Gases Within Cavity	Text, Fig. 7	--	-2000 to +3000

TABLE III

COMPARISON OF PROPERTIES OF VARIOUS MODERATOR COOLANT FLUIDS

Data from Ref. 12

Pressure = 1000 atm Temperature = 4000 R

Fluid	Density ρ Lb/ft^3	ρ / ρ_{REF}	Specific Heat BTU/lb ^{o}R	$C_P/C_{P_{REF}}$	Viscosity μ Lb/sec-ft	μ/μ_{REF}	Prandtl Number Pr	Pr/Pr_{REF}
$H_{2_{Ref}}$	0.69	1.0	4.2	1.0	2.24×10^{-5}	1.0	0.65	1.0
H_2	0.690	1.0	4.137	0.985	2.32×10^{-5}	1.036	0.665	1.023
D_2	1.379	1.999	2.159	0.514	3.20×10^{-5}	1.429	0.667	1.026
H_2O	6.169	8.941	0.698	0.166	5.01×10^{-5}	2.237	0.689	1.060
D_2O	6.858	9.939	0.712	0.170	5.17×10^{-5}	2.308	0.699	1.075
He	1.371	1.987	1.241	0.295	5.13×10^{-5}	2.290	0.635	0.977
CH_4*	5.493	7.961	1.440	0.343	3.56×10^{-5}	1.589	0.669	1.029

* see text

TABLE IV

COMPARISON OF COOLANT FLOW CHARACTERISTICS FOR VARIOUS MODERATOR COOLANT FLUIDS

Flow Characteristics Apply to Moderator with Same

d, V_p, $T_w - T_c$, $\Delta T_c / \Delta X$ and Q_v

FLUID COOLANT	$\frac{Re_d}{Re_{d_{REF}}} = \left(\frac{Pr}{Pr_{Ref}}\right)^{5/6} \frac{(C_p\mu)^{1.25}_{Ref}}{(C_p\mu)^{1.25}}$	$\frac{\Delta\ell/\Delta X}{(\Delta\ell/\Delta X)_{Ref}} = \left(\frac{Pr}{Pr}\right)^{5/6}_{REF} \left(\frac{(C_p\mu)_{REF}}{C_p\mu}\right)^{0.25}$	$\frac{V}{V_{REF}} = \left(\frac{Pr}{Pr_{REF}}\right)^{5/6} \frac{\left(\rho\mu^{0.25} C_p^{1.25}\right)_{REF}}{\rho\mu^{0.25} C_p^{1.25}}$	$\frac{q}{q_{REF}} = \left(\frac{Pr}{Pr_{REF}}\right)^{5/3} \frac{\left(\rho\mu^{0.50} C_p^{2.5}\right)_{REF}}{\rho\mu^{0.50} C_p^{2.5}}$	$\frac{\Delta P/\Delta X}{(\Delta P/\Delta X)_{REF}} = \left(\frac{Pr}{Pr_{REF}}\right)^{7/3} \frac{\left(\rho\mu^{0.50} C_p^{2.5}\right)_{REF}}{\rho\mu^{0.50} C_p^{2.5}}$	
$H_{2_{Ref}}$	1.0	1.0	1.0	1.0	1.0	
H_2	0.994	1.014	1.053	1.060	1.077	
D_2	1.502	1.104	1.805	3.239	3.317	
H_2O	3.623	1.345	4.684	3.722	4.020	
D_2O	3.421	1.343	4.468	3.691	3.873	
He	1.602	1.082	3.084	6.118	6.022	
CH_4 *	2.187	1.192	2.070	3.853	3.926	

* See Text

TABLE V

SPECIFIC IMPULSE OBTAINABLE FROM GASEOUS NUCLEAR ROCKETS USING DIFFERENT PROPELLANTS

No Space Radiator

$C_N = 0.80$

Propellant	H_W at $T = 5300^\circ R$ BTU/lb	$H_{EXIT} = 10\ H_W$ BTU/lb	I_{SP}, sec
H_2	20,000	200,000	2500
CH_4	10,000	100,000	1800
NH_3	6700	67,000	1450
H_2O	4600	46,000	1200
50% H_2, 50% H_2O	12,300	123,000	1960

LOCATION OF MODERATOR-REFLECTOR IN POSSIBLE GASEOUS NUCLEAR ROCKET ENGINE CONFIGURATION

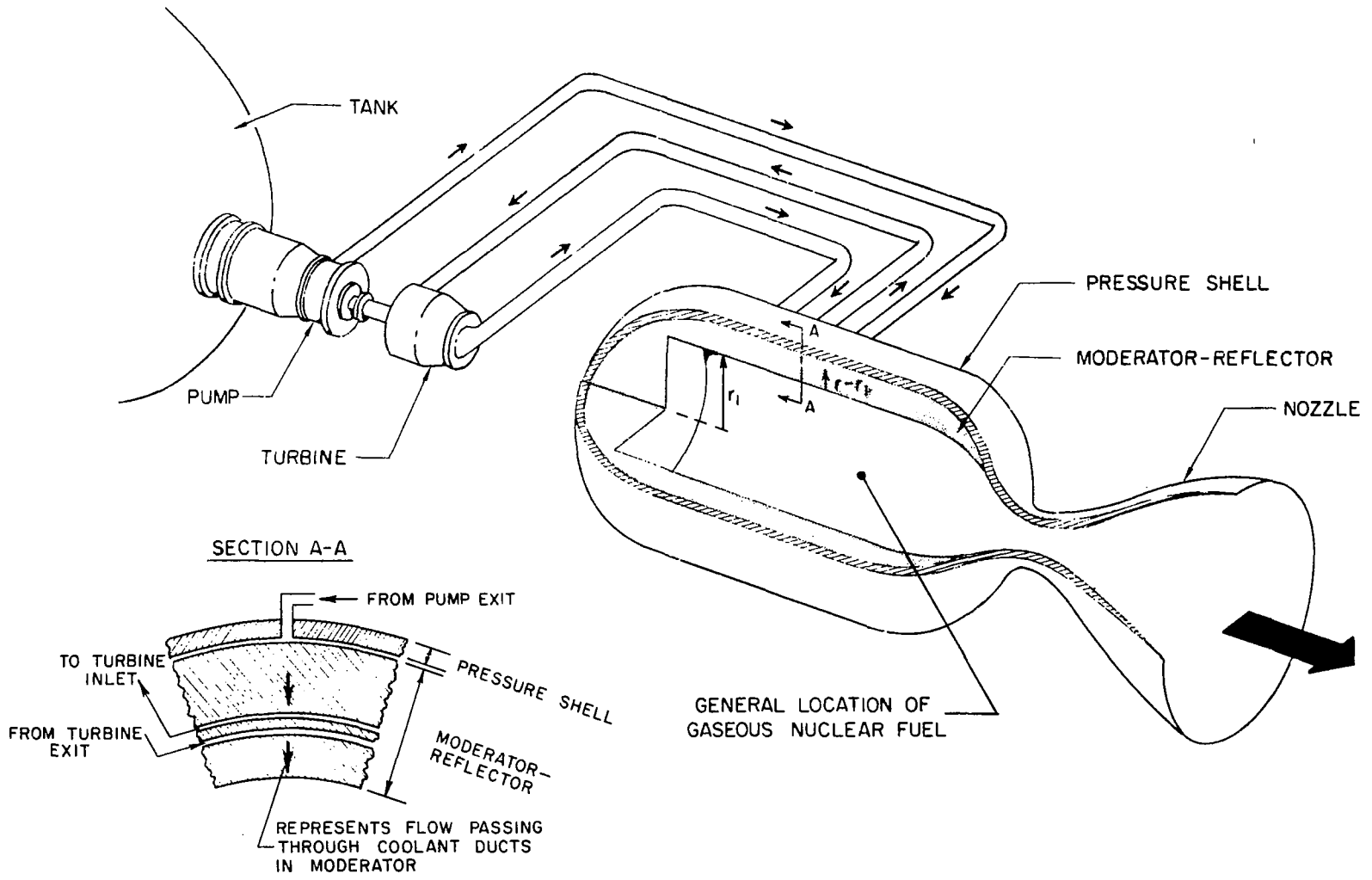

Figure 1

Figure 2

REFERENCE GASEOUS NUCLEAR ROCKET ENGINE CONFIGURATION EMPLOYED IN ANALYSES

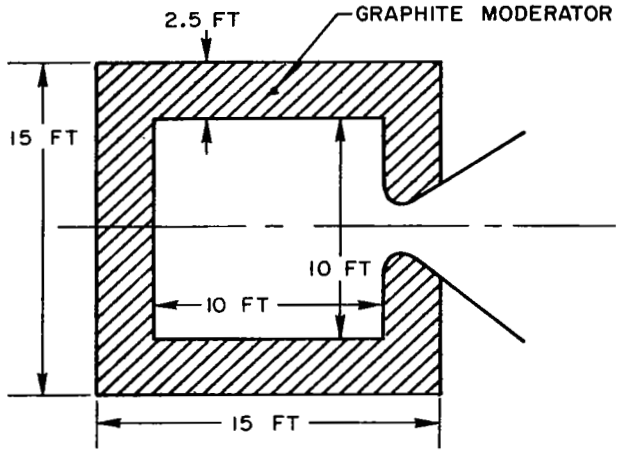

Cavity surface area	471 ft^2
Cavity volume	785 ft^3
Moderator volume	1860 ft^3
Moderator density	100 lb/ft^3
Moderator weight	186,000 lb
Total engine weight	300,000 lb
Unit power	10^6 BTU/sec-ft^2 of cavity surface
Total power	4.71×10^8 BTU/sec = 496,000 mw
Specific impulse	2500 sec
Exit enthalpy corresponding to specific impulse	200,000 BTU/lb
Propellant flow	2350 lb/sec
Thrust	5.88×10^6 lb
Thrust/(engine weight)	19.6

Figure 3

ENERGY FLOW AND ENERGY DEPOSITION RATE IN GRAPHITE MODERATOR-REFLECTOR DUE TO NEUTRONS AND GAMMA RAYS

DATA OBTAINED FROM REF. 5

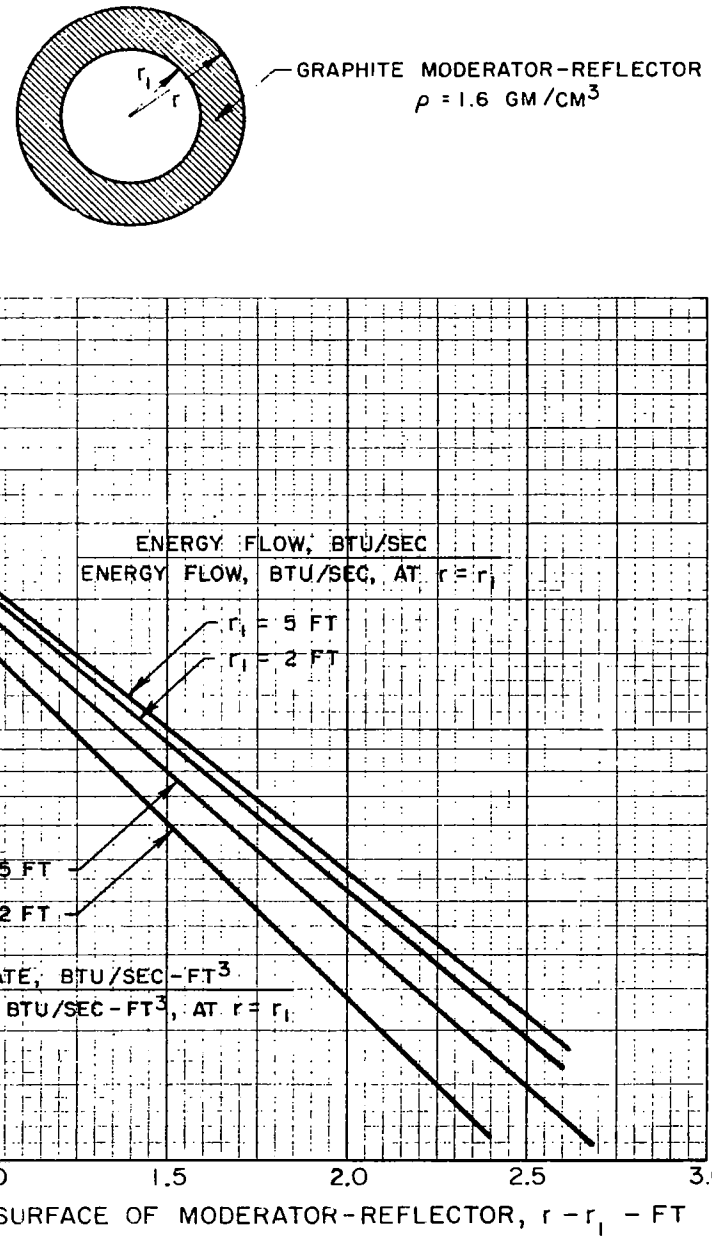

Figure 4

EFFECT OF MODERATOR MATERIAL ON VARIATION OF ENERGY FLOW DUE TO NEUTRONS AND GAMMA RAYS WITH DISTANCE THROUGH MODERATOR

DATA OBTAINED FROM REF. 5

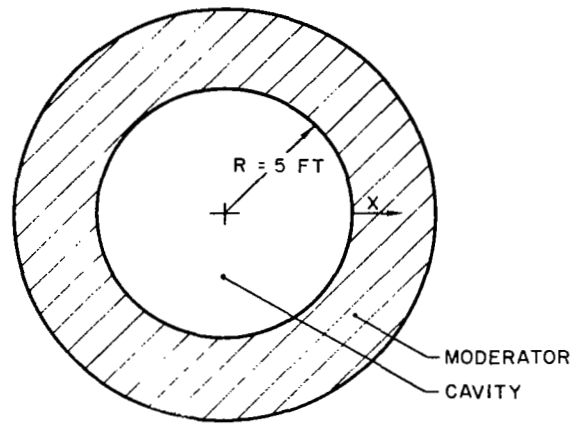

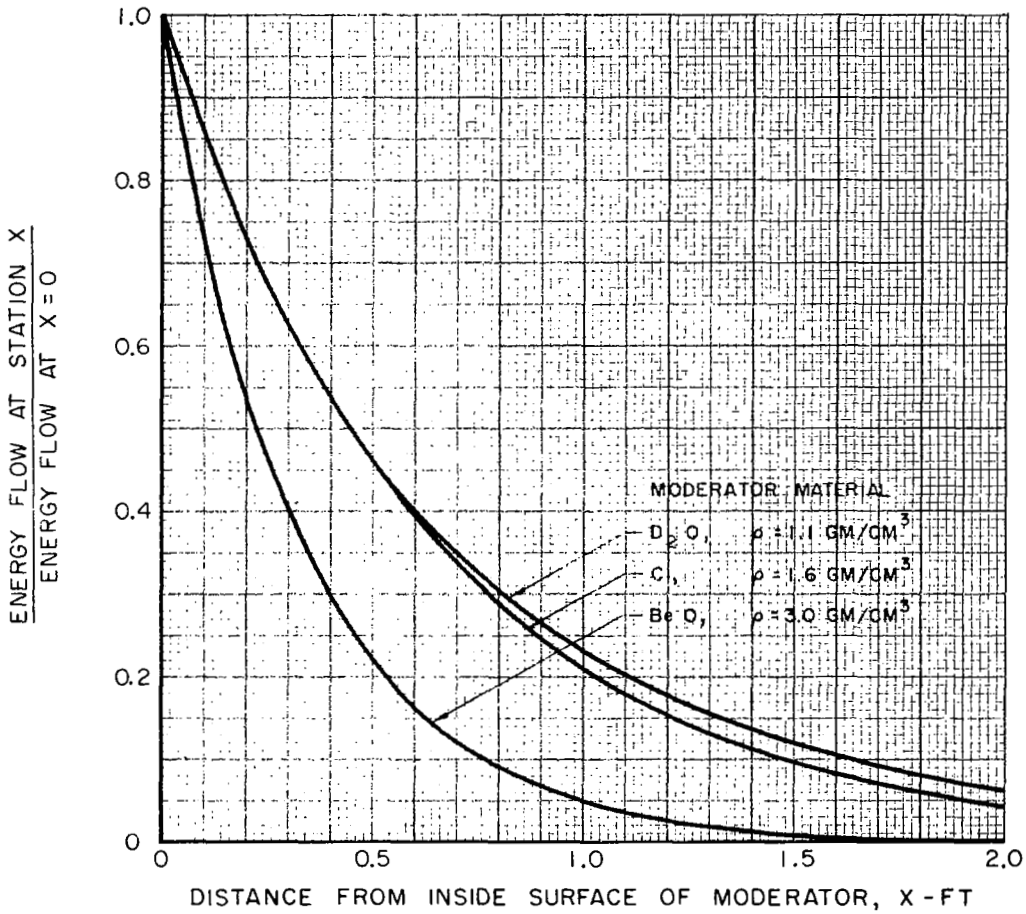

Figure 5

THICKNESS OF SEEDED HYDROGEN LAYER ACQUIRED TO ATTENUATE RADIANT ENERGY

$$\frac{I}{I_0} = \frac{1}{e^{a_e X_s}} = \frac{1}{e^{b_e \rho_s X_s}}$$

TO MAKE $I/I_0 = 10^{-3}$, $b_e \rho_s X_s = 6.91$; THEREFORE $X_s = 6.91 / b_e \rho_s$

b_e ASSUMED TO BE 8,000 CM^2/GM (SEE TEXT)

SEED DENSITY, ρ_s, ASSUMED TO BE 1% OF HYDROGEN DENSITY

HYDROGEN DENSITY FROM REF. 7

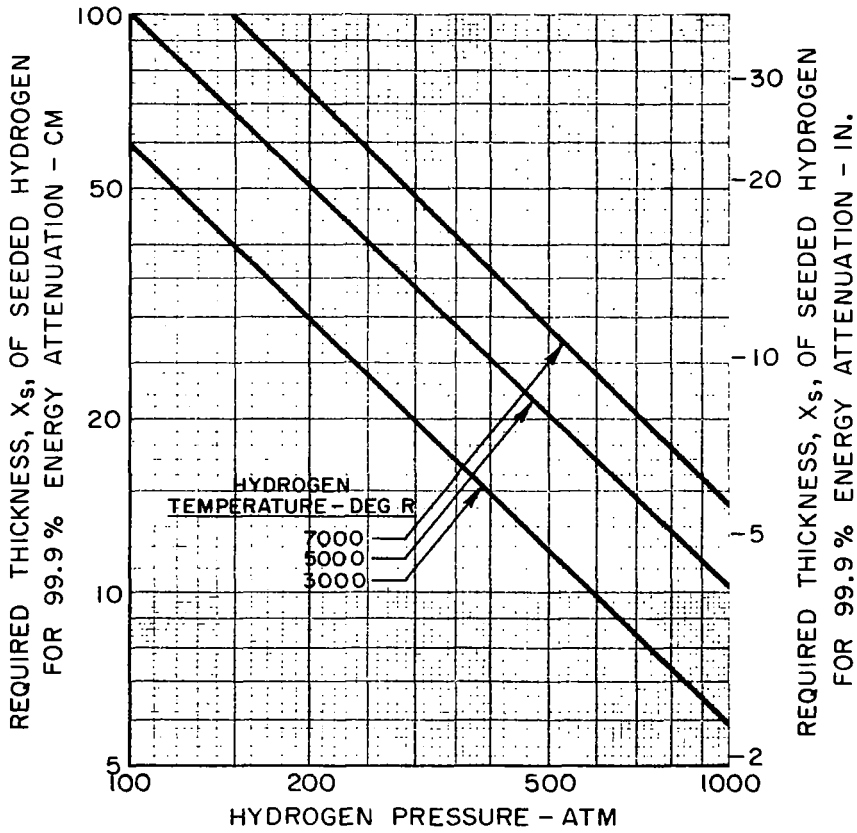

Figure 6

TEMPERATURE DISTRIBUTION ASSUMED NEAR MODERATOR SURFACE

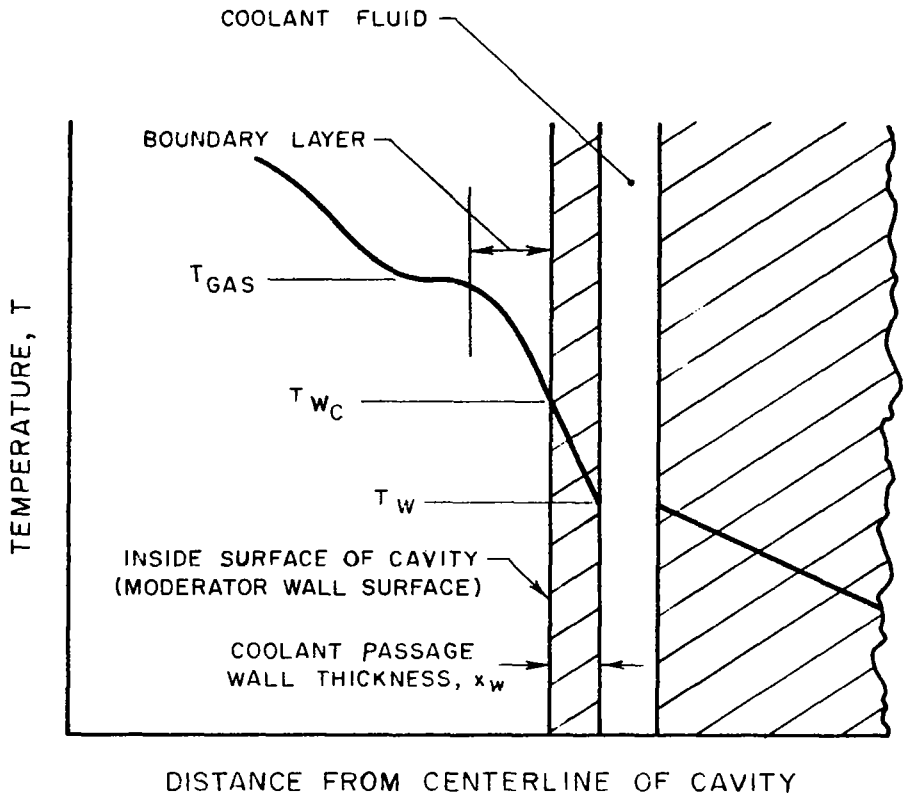

Figure 7

EFFECT OF GAS TEMPERATURE AND VELOCITY ON CONVECTIVE HEAT TRANSFER TO CAVITY WALL

CAVITY WALL TEMPERATURE, T_{WC} = 5000 R

HYDROGEN PRESSURE = 500 ATM

STANTON NUMBER, St = 0.0012

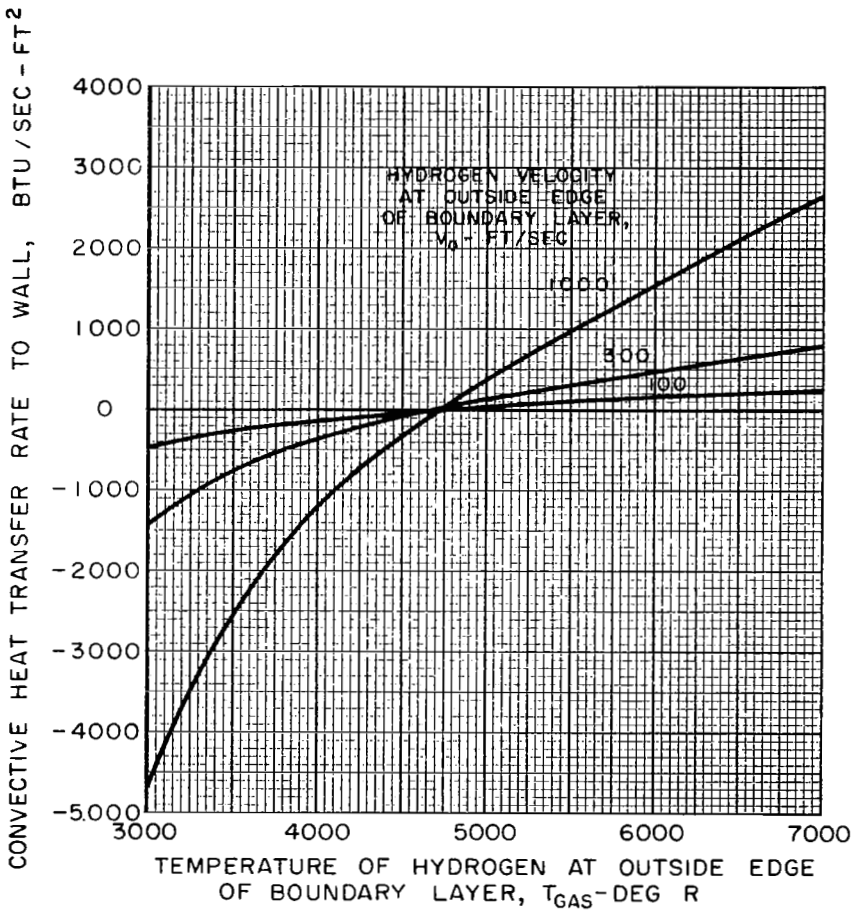

Figure 8

MODERATOR COOLANT FLOW DIAGRAMS WITH INWARD COOLANT FLOW

a – DIRECT COOLING WITH PROPELLANT FLOW

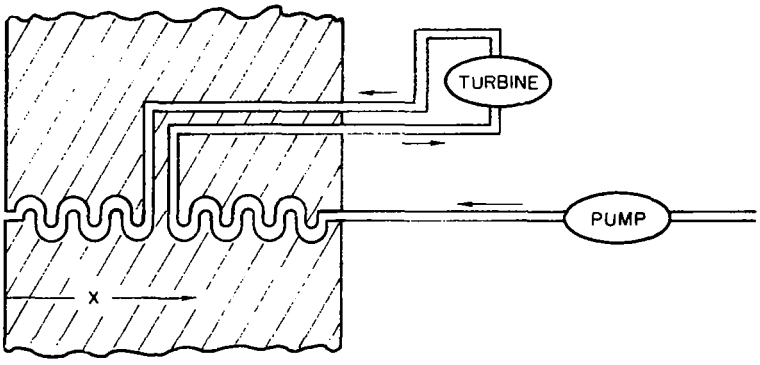

b – PARTIAL COOLING USING AUXILIARY COOLANT LOOP

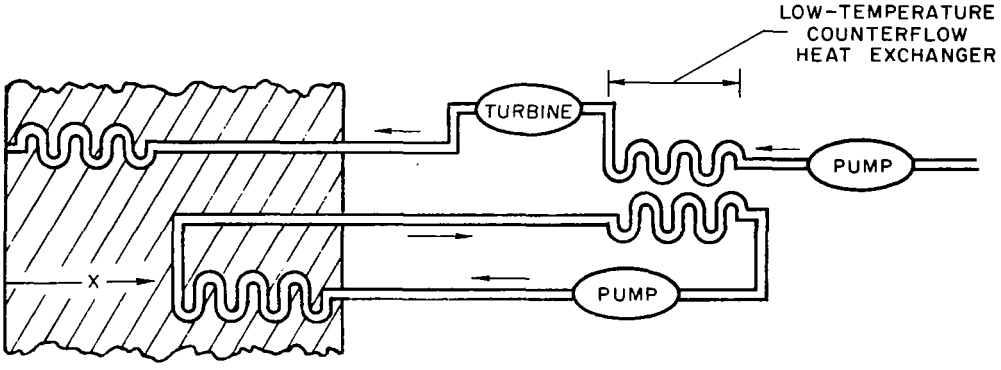

c – FULL COOLING USING AUXILIARY COOLANT LOOP

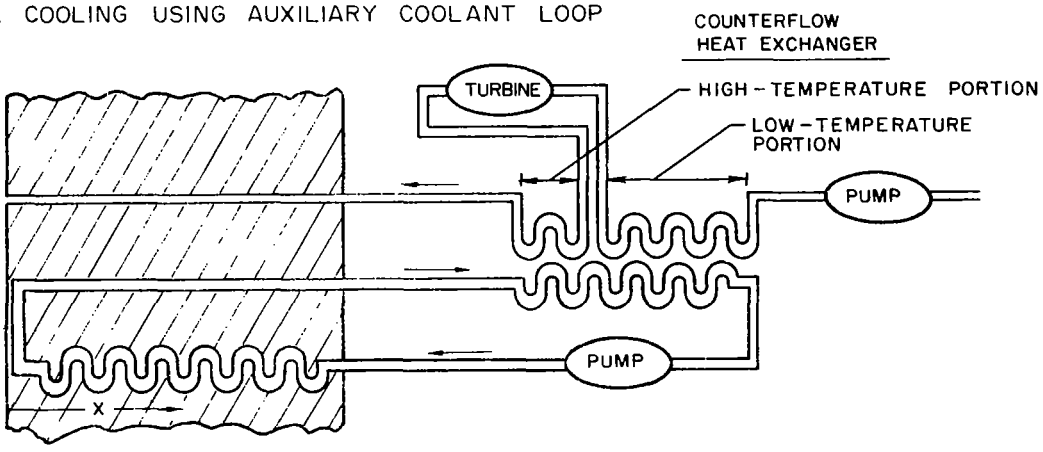

EFFECT OF TURBINE EXIT PRESSURE ON REQUIRED TURBINE PRESSURE DROP

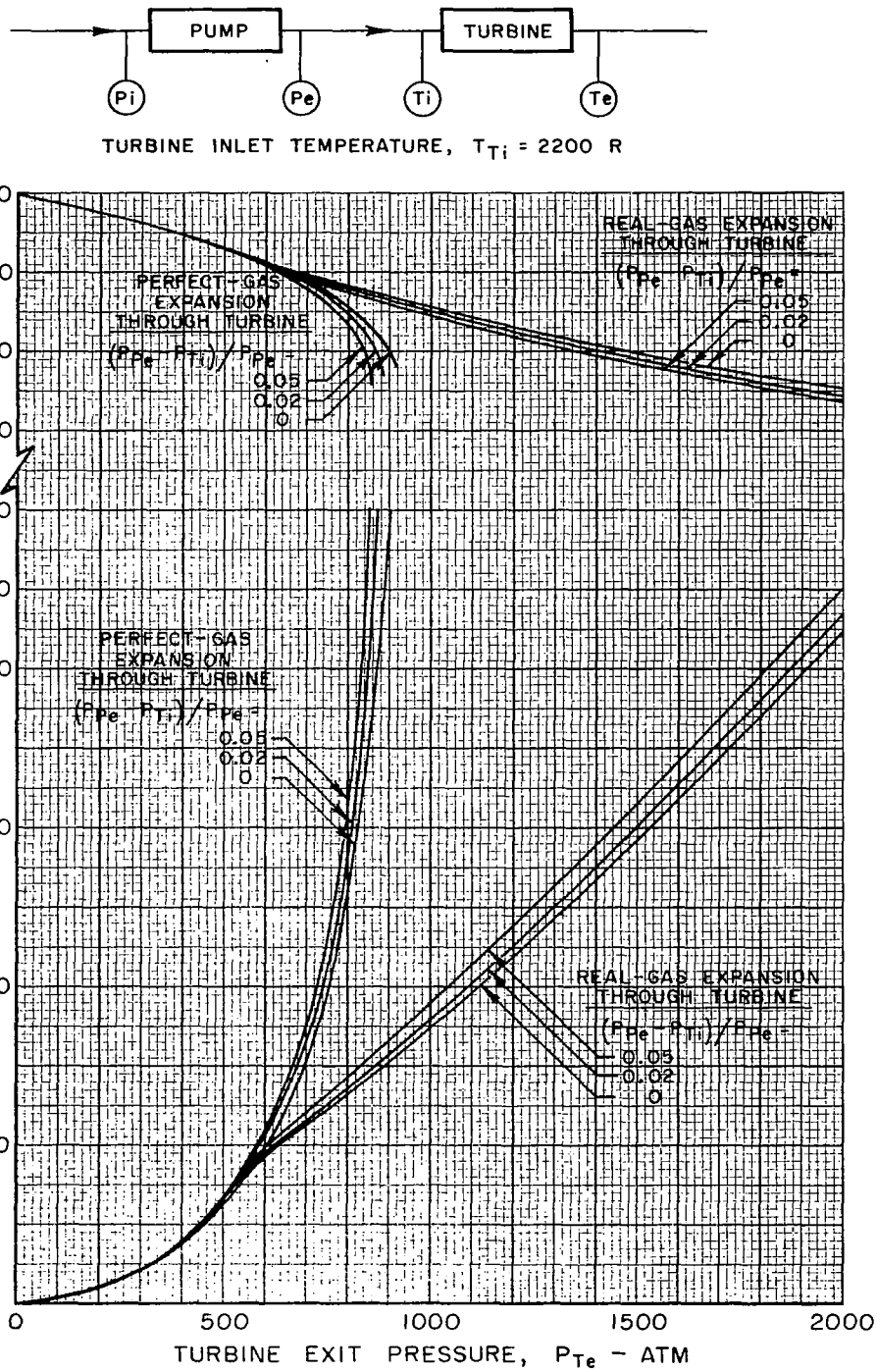

Figure 10

TYPICAL TEMPERATURE AND PRESSURE DISTRIBUTIONS IN GRAPHITE MODERATOR – REFLECTOR

CALCULATED FROM HEAT FLOW CURVES IN FIG. 3
FOR NEUTRON AND GAMMA RAYS AND FOR r_1 = 5 FT

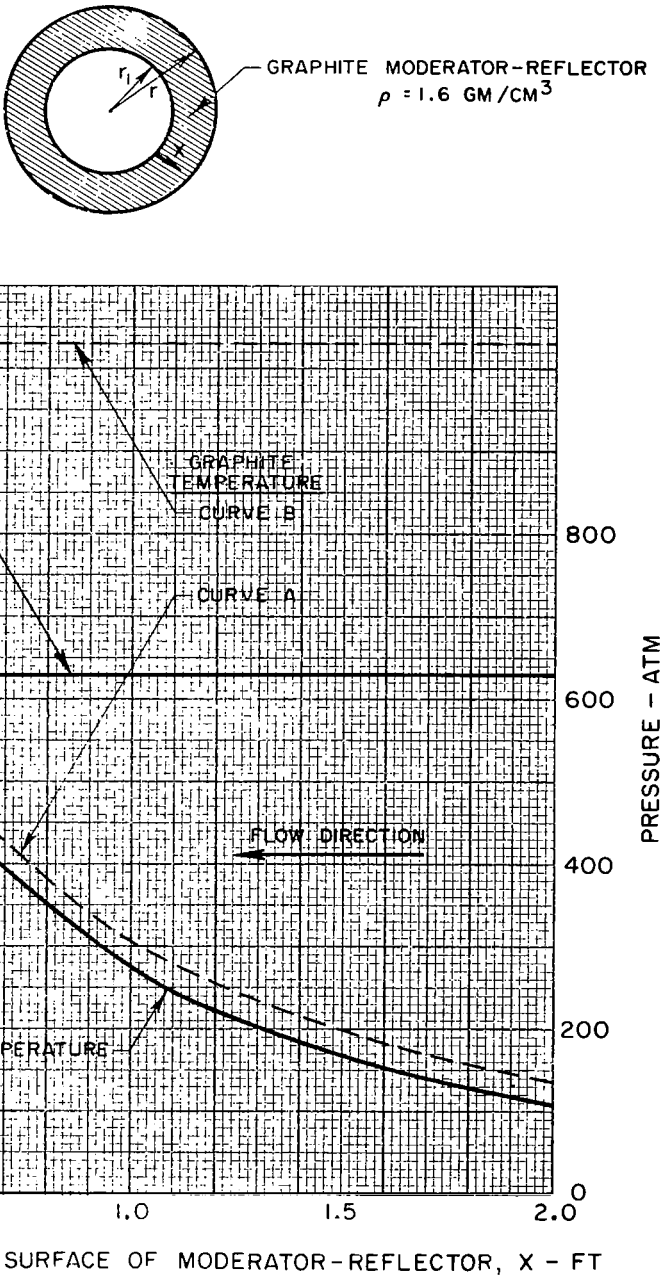

TYPICAL COOLANT TEMPERATURE DISTRIBUTIONS IN MODERATOR WITH INWARD COOLANT FLOW

CURVE	LOCAL MODERATOR MATERIAL	RANGE OF X, FT	
		$T_{c\,MAX}$ = 5000 R	$T_{c\,MAX}$ = 3000 R
A	C	0 → 2.50	0 → 2.50
B	C	0 → 1.00	0 → 0.71
	D_2O	1.03 → 2.50	0.71 → 2.50
C	C	0 → 0.33	—
	BeO	0.33 → 2.50	0 → 2.50
D	C	0 → 0.33	→
	BeO	0.33 → 0.69	0 → 0.36
	D_2O	0.69 → 2.50	0.36 → 2.50

SYMBOL O INDICATES INTERFACE BETWEEN DIFFERENT MODERATOR REGIONS

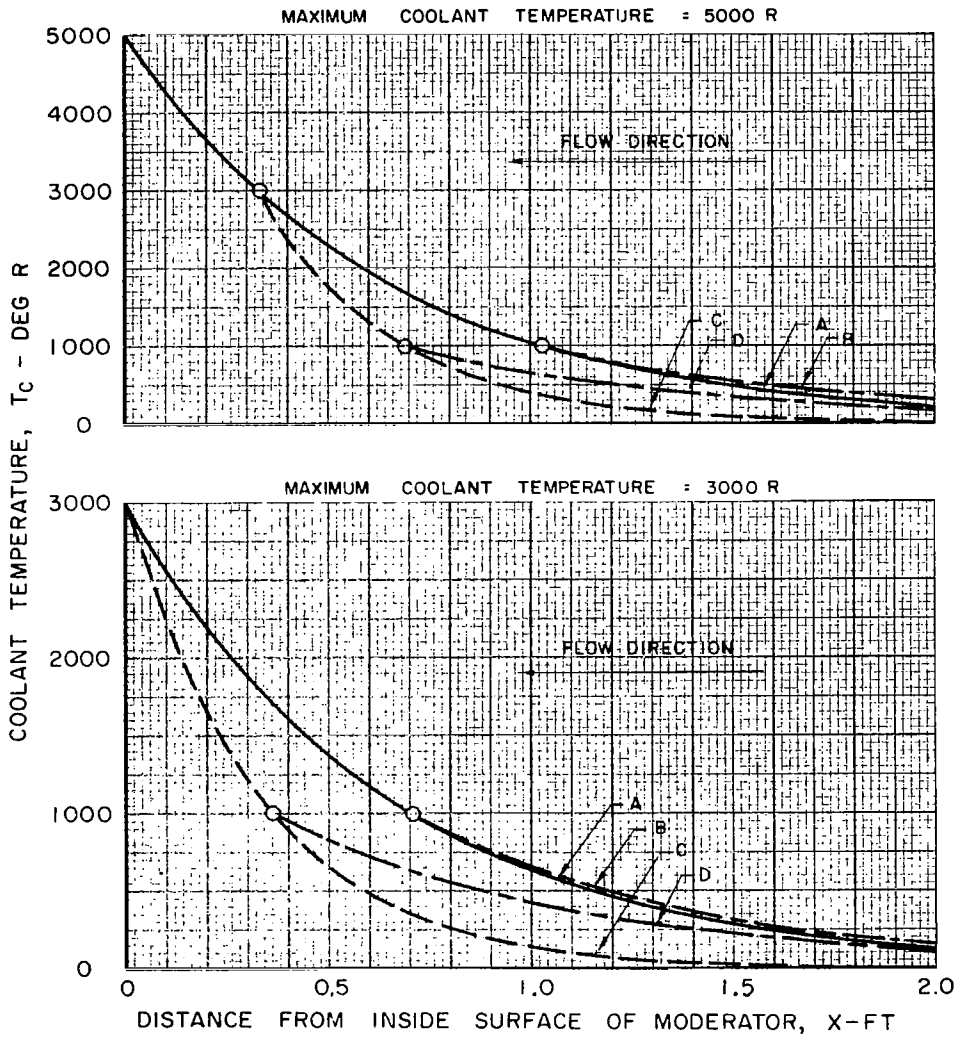

Figure 12

EFFECT OF MODERATOR TEMPERATURE AND PRESENCE OF HYDROGEN COOLANT ON MACROSCOPIC MODERATOR ABSORPTION COEFFICIENT

MODERATOR MATERIAL - GRAPHITE

P_H = HYDROGEN PRESSURE, ATM

$$V_P = \frac{\text{COOLANT DUCT VOLUME}}{\text{VOLUME OF GRAPHITE + COOLANT DUCTING}}$$

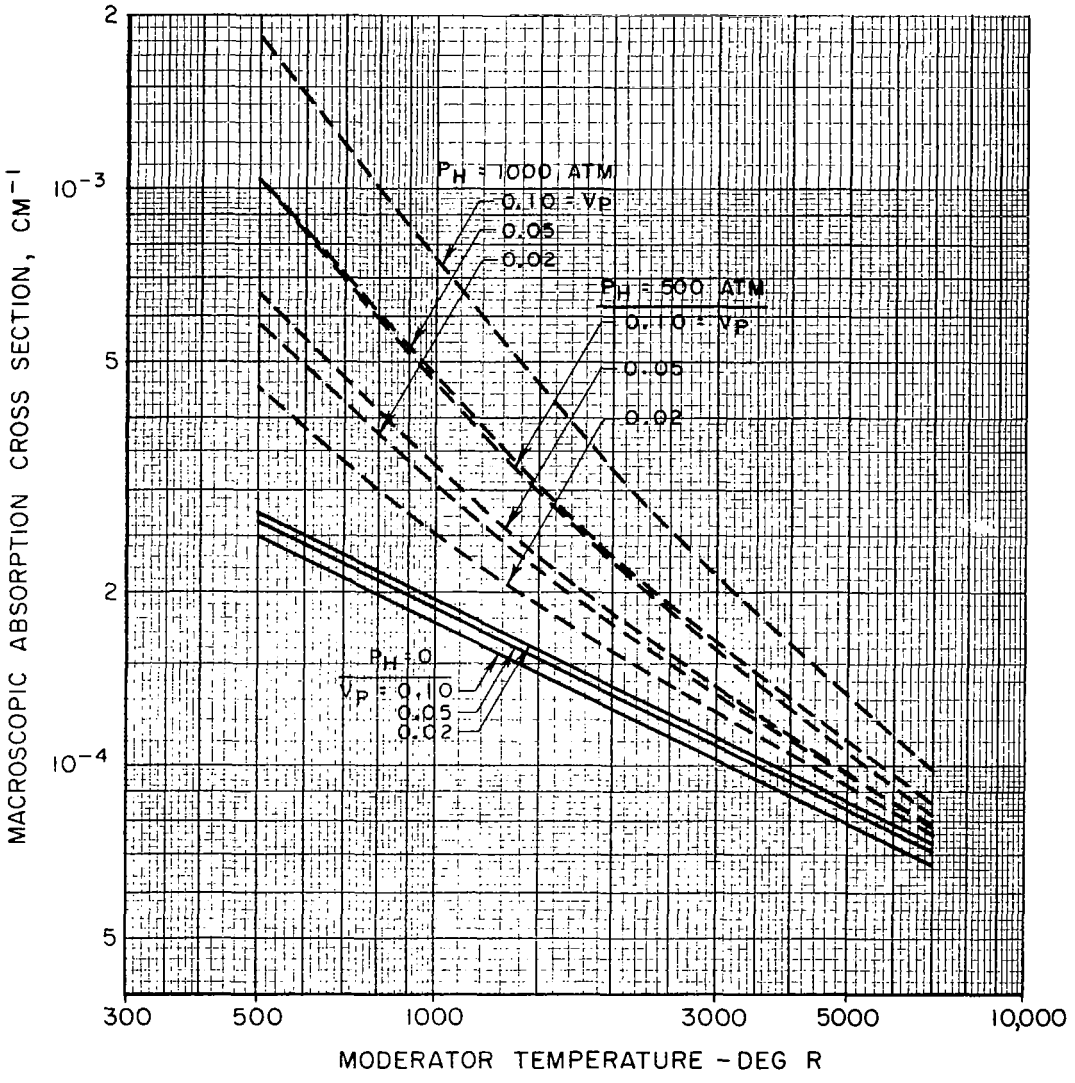

Figure 13

MODERATOR COOLANT FLOW DIAGRAMS WITH OUTWARD COOLANT FLOW

a - DIRECT COOLING WITH PROPELLANT FLOW

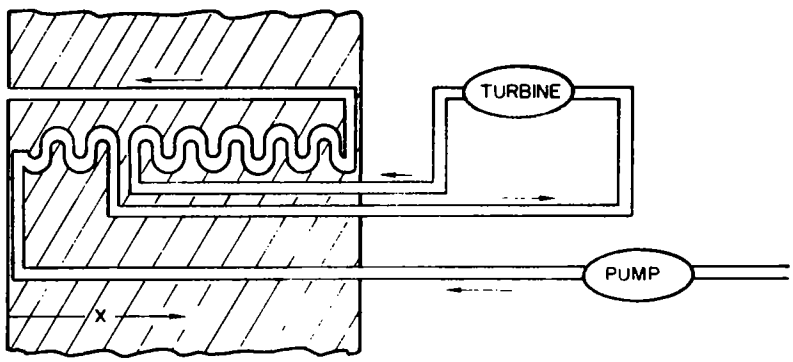

b - FULL COOLING USING AUXILIARY COOLANT LOOP

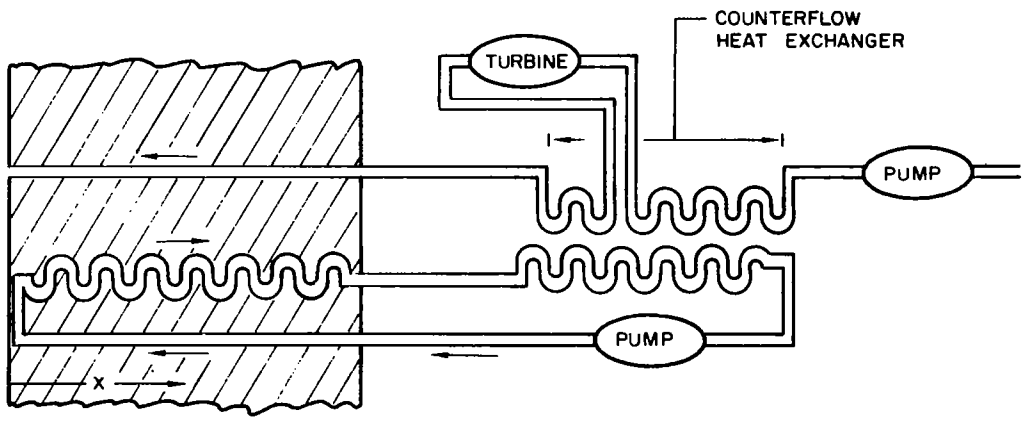

Figure 14

TYPICAL COOLANT TEMPERATURE DISTRIBUTIONS IN MODERATOR WITH OUTWARD COOLANT FLOW

CURVE	LOCAL MODERATOR MATERIAL	RANGE OF X, FT	
		$T_{c\,MAX}$ = 5000 R	$T_{c\,MAX}$ = 3000 R
A	C	0 → 2.50	0 → 2.50
B	D_2O	0 → 0.15	0 → 0.26
	C	0.15 → 2.50	0.26 → 2.50
C	D_2O	0 → 0.15	0 → 0.26
	Be O	0.15 → 0.37	0.26 → 2.50
	C	0.37 → 2.50	—
D	Be O	0 → 0.30	0 → 2.50
	C	0.30 → 2.50	—

SYMBOL O INDICATES INTERFACE BETWEEN DIFFERENT MODERATOR REGIONS

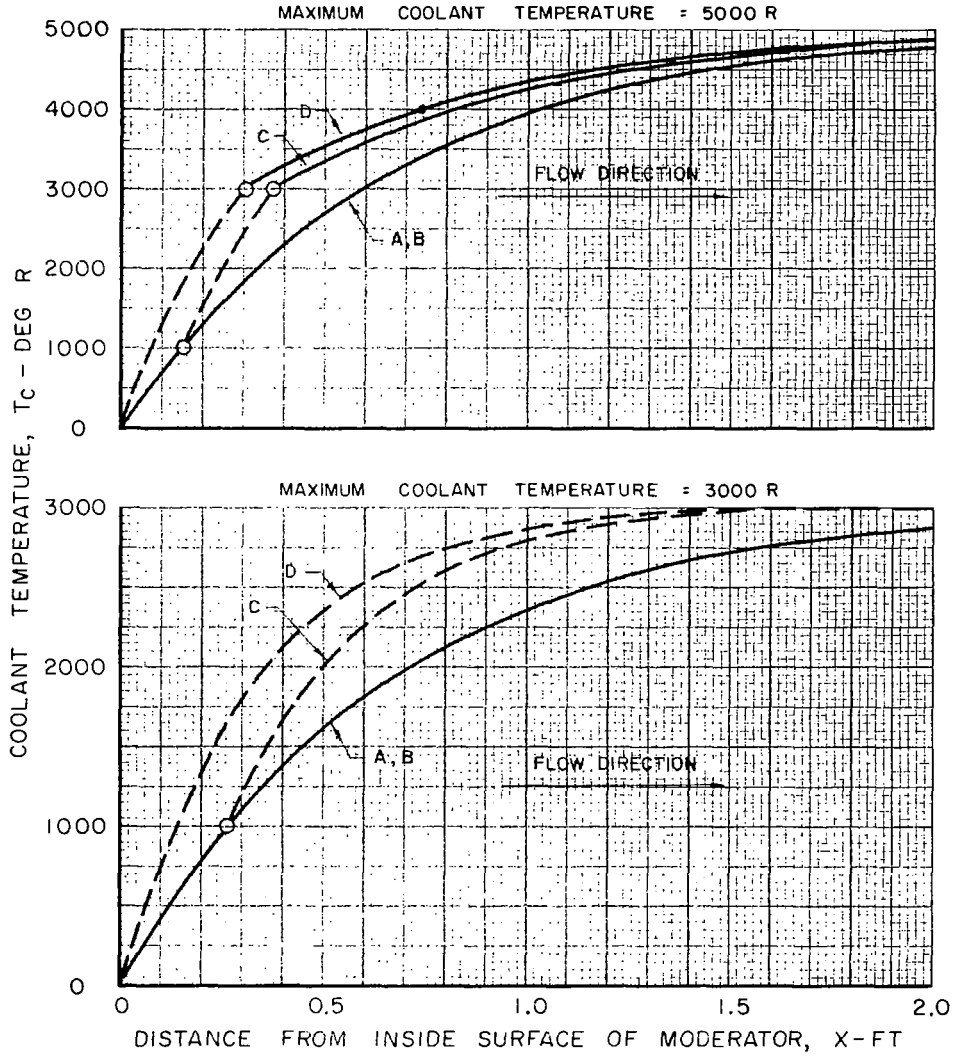

MODERATOR COOLANT FLOW DIAGRAMS WITH COMBINATION OF INWARD AND OUTWARD COOLANT FLOW

a – DIRECT COOLING WITH PROPELLANT FLOW

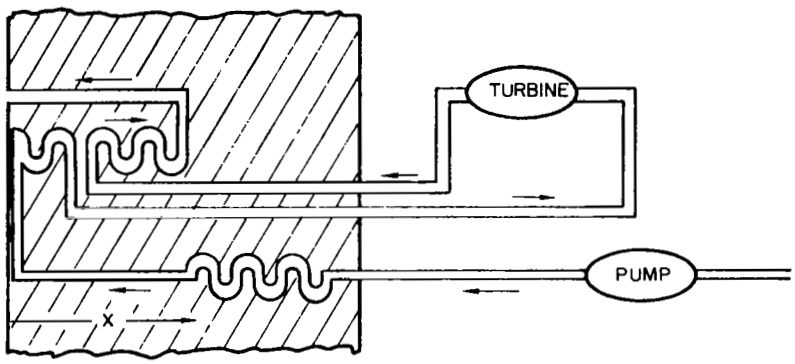

b – FULL COOLING USING AUXILIARY COOLANT LOOP

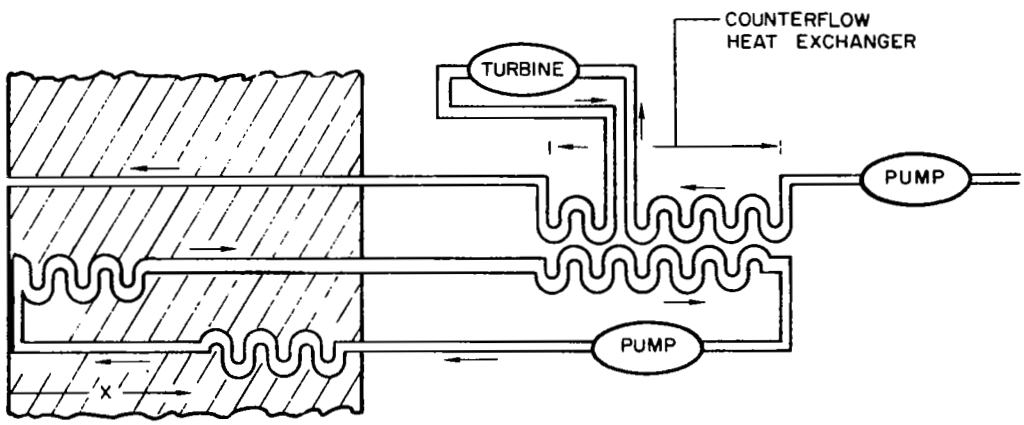

Figure 16

TYPICAL COOLANT TEMPERATURE DISTRIBUTIONS IN MODERATOR WITH COMBINATION OF INWARD AND OUTWARD COOLANT FLOW

SYMBOL O INDICATES INTERFACE BETWEEN DIFFERENT MODERATOR REGIONS

LOCAL MODERATOR MATERIAL	RANGE OF X, FT	
	$T_{c\,MAX}$ = 5000 R	$T_{c\,MAX}$ = 3000 R
BeO	0 → 0.18	0 → 0.36
C	0.18 → 0.88	—
D_2O	0.88 → 2.50	0.36 → 2.50

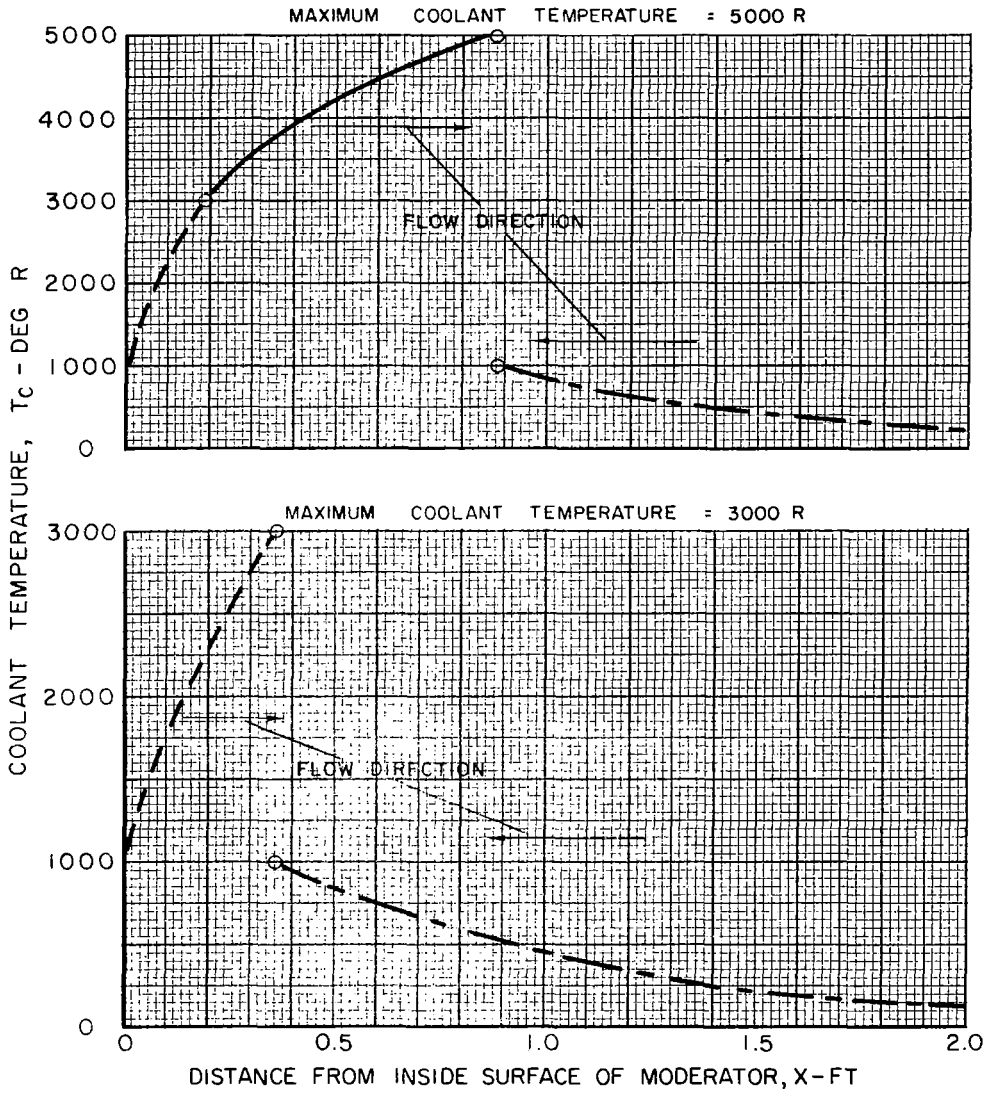

EFFECT OF COOLANT PASSAGE VOLUME FRACTION ON TEMPERATURE DIFFERENCE WITHIN GRAPHITE MODERATOR

RELATION FOR TEMPERATURE DIFFERENCE DETERMINED FROM REF. 16 FOR A TRIANGULAR ARRAY OF COOLANT PASSAGES

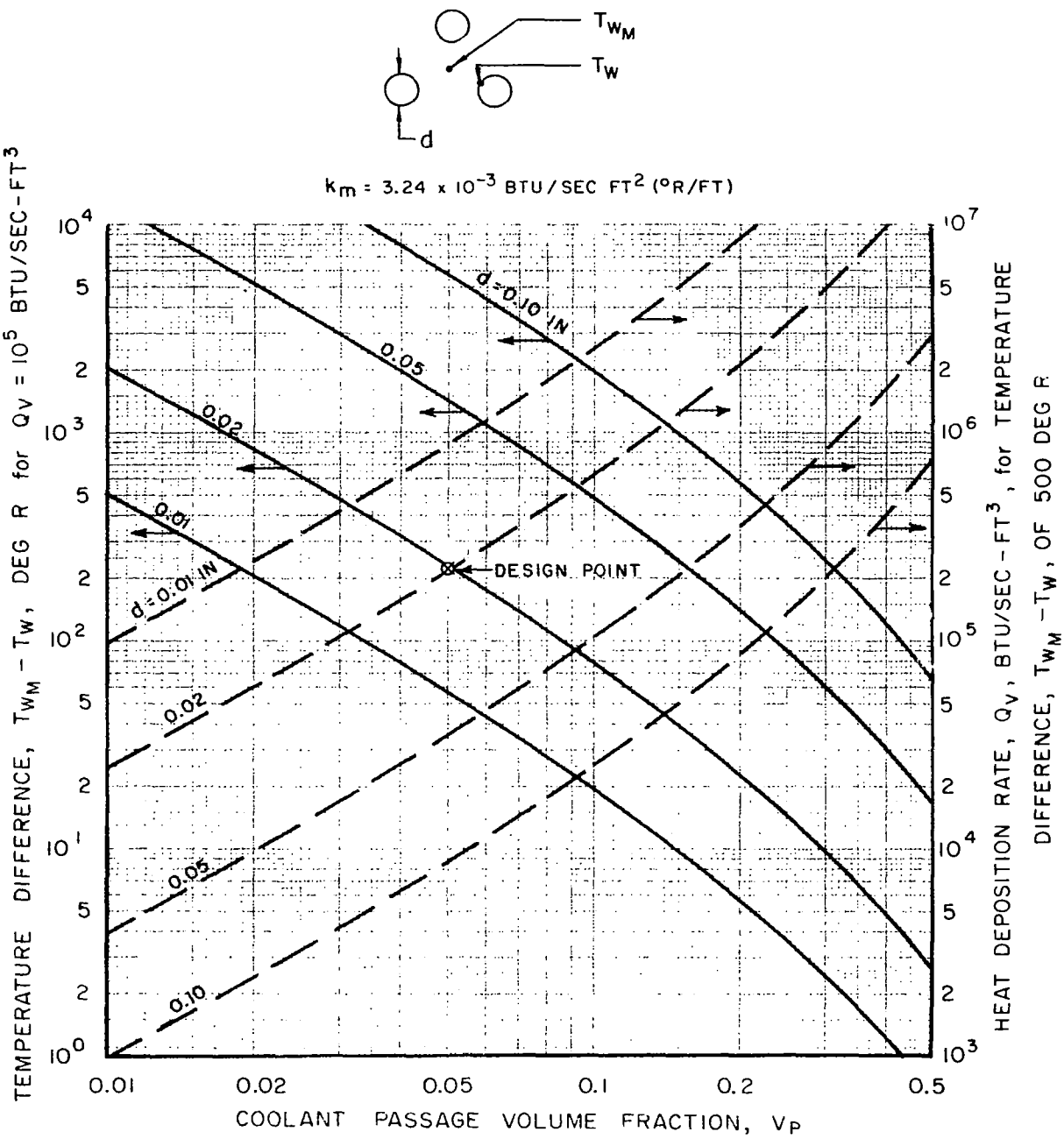

Figure 18

EFFECT OF COOLANT PASSAGE VOLUME FRACTION ON INTERNAL SURFACE AREA OF COOLANT PASSAGES

VALUES OF Q_V ON DASHED CURVES DETERMINED FROM FIG. 17 FOR $T_{W_M} - T_W = 500$ R

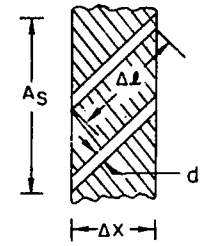

$$\left(\frac{\Delta A_W}{A_S}\right)\Big/\Delta X = \frac{4V_P}{d}$$

$$\Delta A_W = N\pi d\,\Delta\ell$$

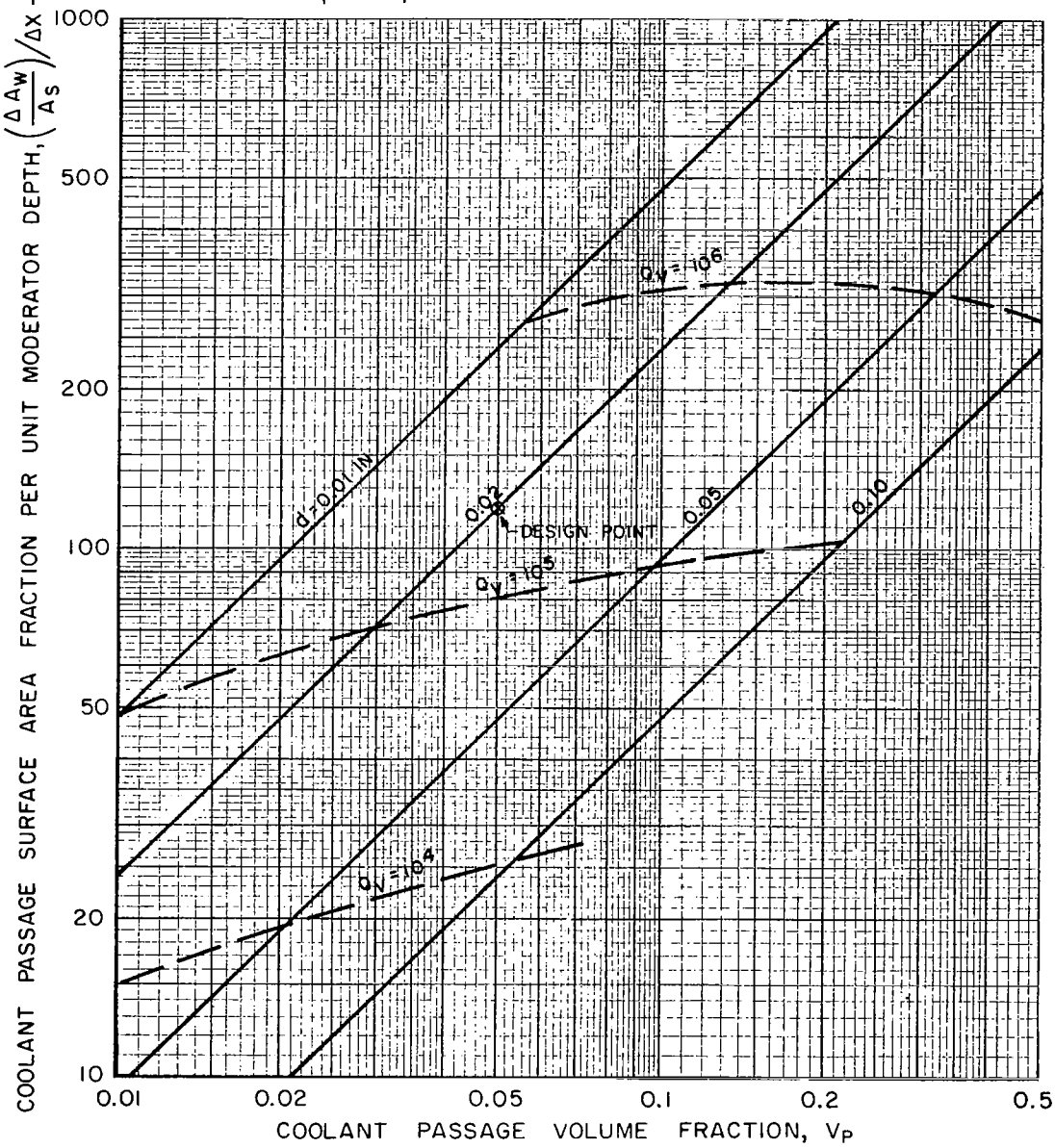

EFFECT OF COOLANT PASSAGE VOLUME FRACTION ON NUMBER OF COOLANT PASSAGES PER UNIT SURFACE AREA

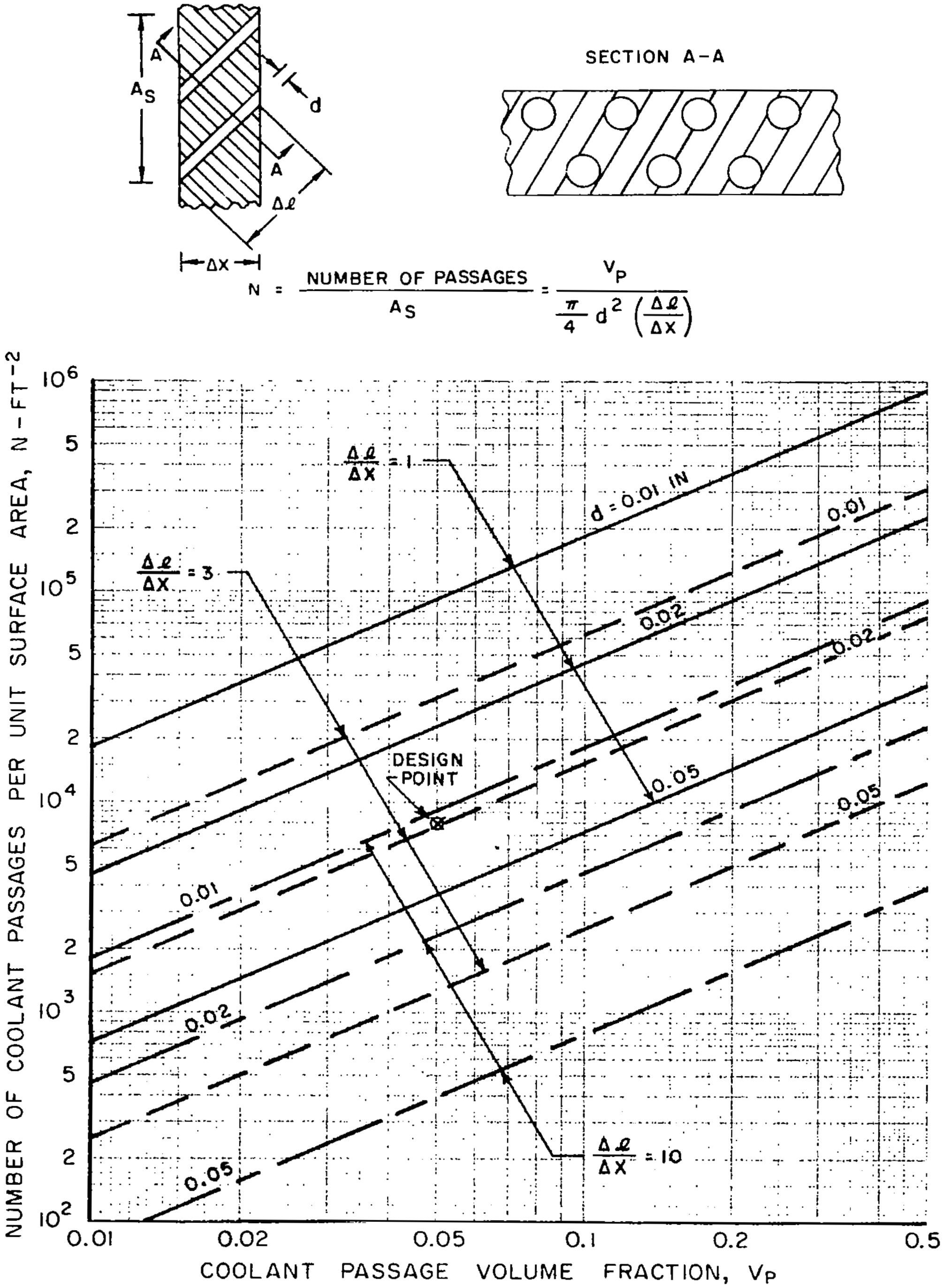

Figure 20

EFFECT OF HEAT DEPOSITION RATE IN MODERATOR ON REYNOLDS NUMBER IN COOLANT PASSAGES

TEMPERATURE DIFFERENCE, $T_W - T_C$ = 200 R
HYDROGEN TEMPERATURE, T_C = 4000 R
HYDROGEN PROPERTIES GIVEN IN TEXT
REYNOLDS NUMBER INDEPENDENT OF GAS PRESSURE

X INDICATES REYNOLDS NUMBER OF 5000
O INDICATES $T_{W_M} - T_W$ = 500 DEG R (SEE FIG. 17)

$$Re_d = \frac{Pr^{5/6}}{0.0507} d^{2.5} \left(\frac{Q_V}{v_P C_P \mu (T_W - T_C)} \right)^{1.25} \qquad \text{EQ. (8)}$$

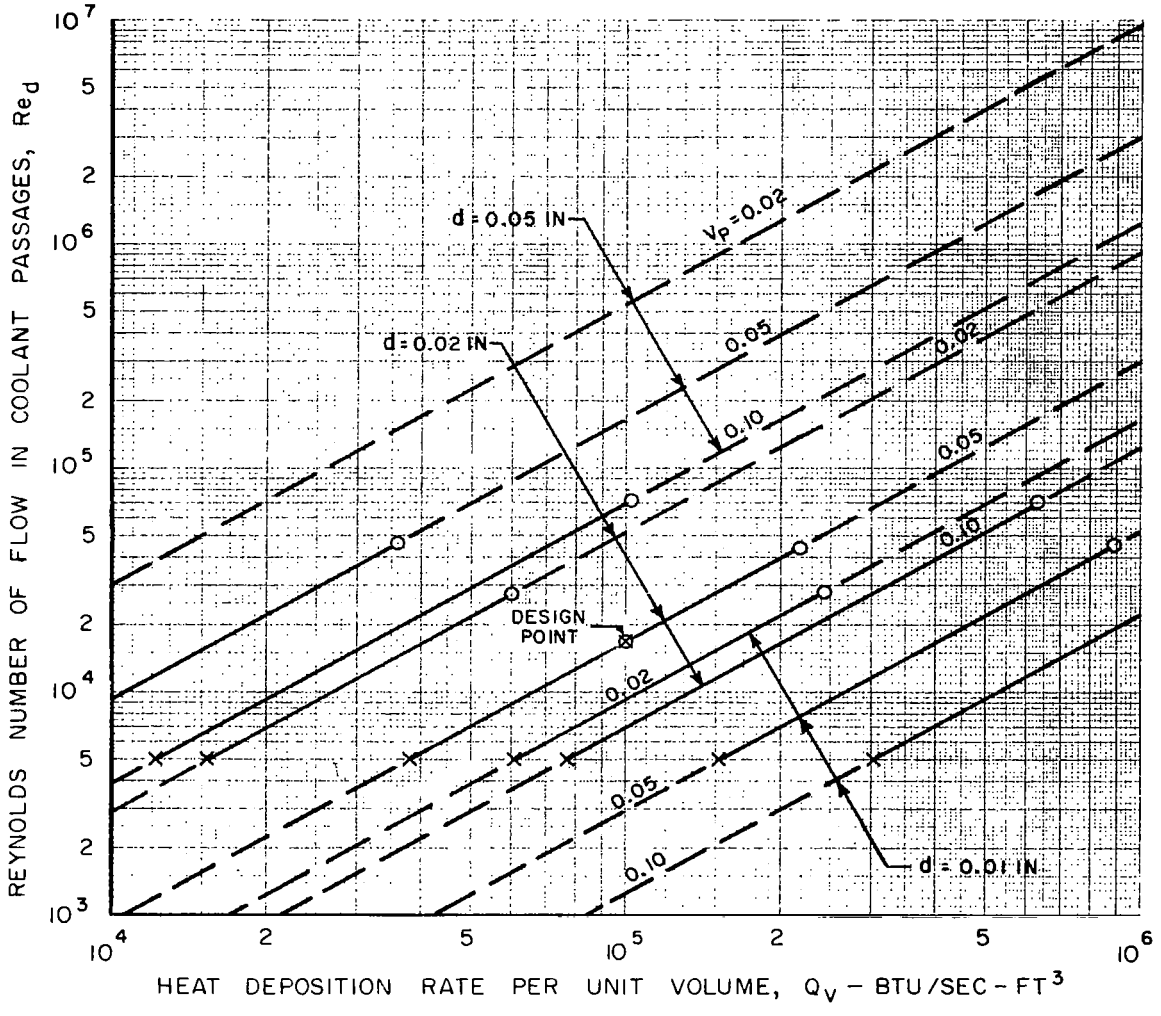

EFFECT OF HEAT DEPOSITION RATE IN MODERATOR ON SLOPE OF COOLANT PASSAGES

TEMPERATURE DIFFERENCE, $T_W - T_C$ = 200 R
COOLANT TEMPERATURE GRADIENT, $\Delta T_C/\Delta X$ = 6000 R/FT
HYDROGEN TEMPERATURE, T_C = 4000 R
HYDROGEN PROPERTIES GIVEN IN TEXT
PASSAGE SLOPE INDEPENDENT OF GAS PRESSURE

× INDICATES REYNOLDS NUMBER OF 5000
○ INDICATES $T_{W_M} - T_W$ = 500 DEG R (SEE FIG. 17)

$$\frac{\Delta \ell}{\Delta X} = \frac{d^{1.5} Pr^{5/6}}{0.0507 (T_W - T_C)^{1.25}} \frac{\Delta T_C}{\Delta X} \left(\frac{Q_V}{V_P C_P \mu} \right)^{0.25} \qquad \text{EQ. (15)}$$

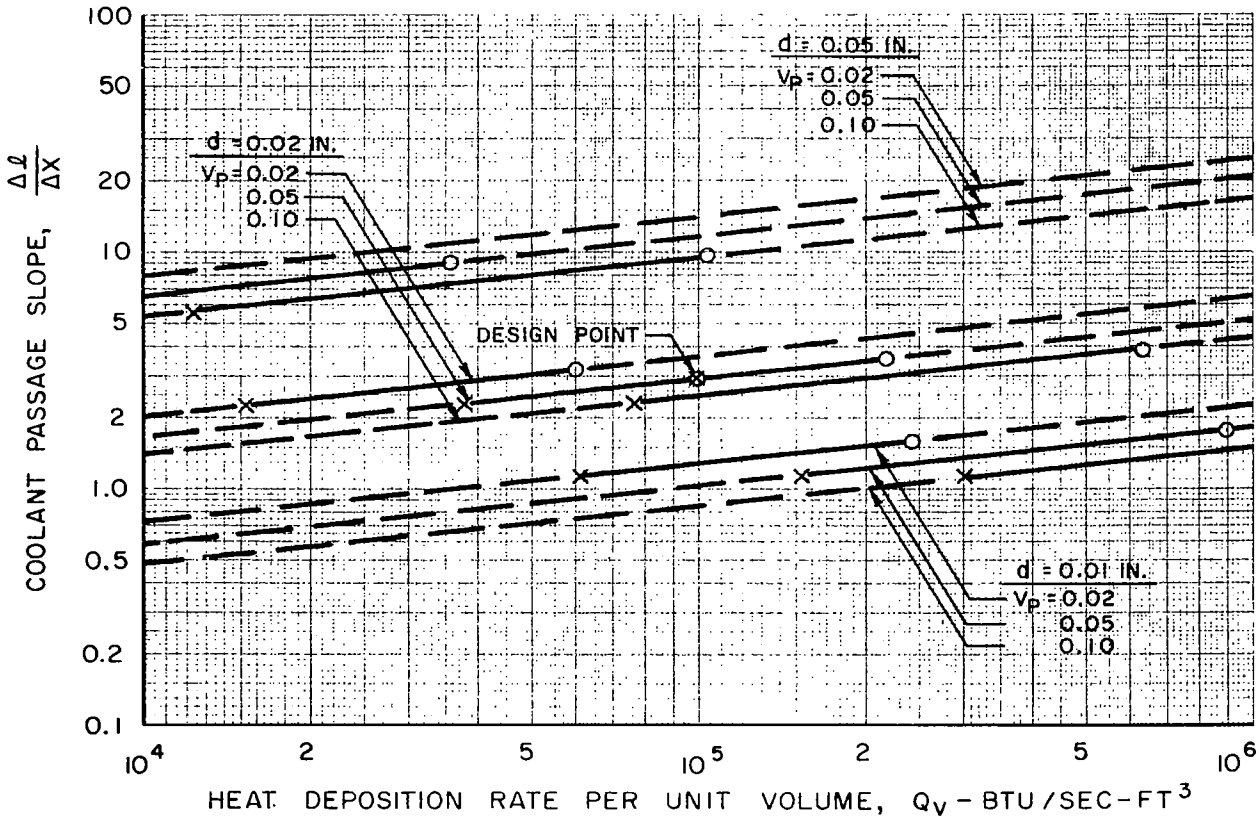

Figure 22

EFFECT OF HEAT DEPOSITION RATE IN MODERATOR ON VELOCITY IN COOLANT PASSAGES

TEMPERATURE DIFFERENCE, $T_W - T_C$ = 200 R
COOLANT TEMPERATURE GRADIENT, $\Delta T_C/\Delta X$ = 6000 R/FT
HYDROGEN TEMPERATURE, T_C = 4000 R
HYDROGEN PROPERTIES GIVEN IN TEXT
PRESSURE = 1000 ATM (VELOCITY INVERSELY PROPORTIONAL TO PRESSURE)

× INDICATES REYNOLDS NUMBER OF 5000
O INDICATES $T_{W_M} - T_W$ = 500 DEG R (SEE FIG. 17)

$$V = \frac{d^{1.5}\, Pr^{5/6}}{0.0507\, \rho\, \mu^{0.25}} \left(\frac{Q_V}{V_P C_P (T_W - T_C)} \right)^{1.25} \qquad \text{EQ. (16)}$$

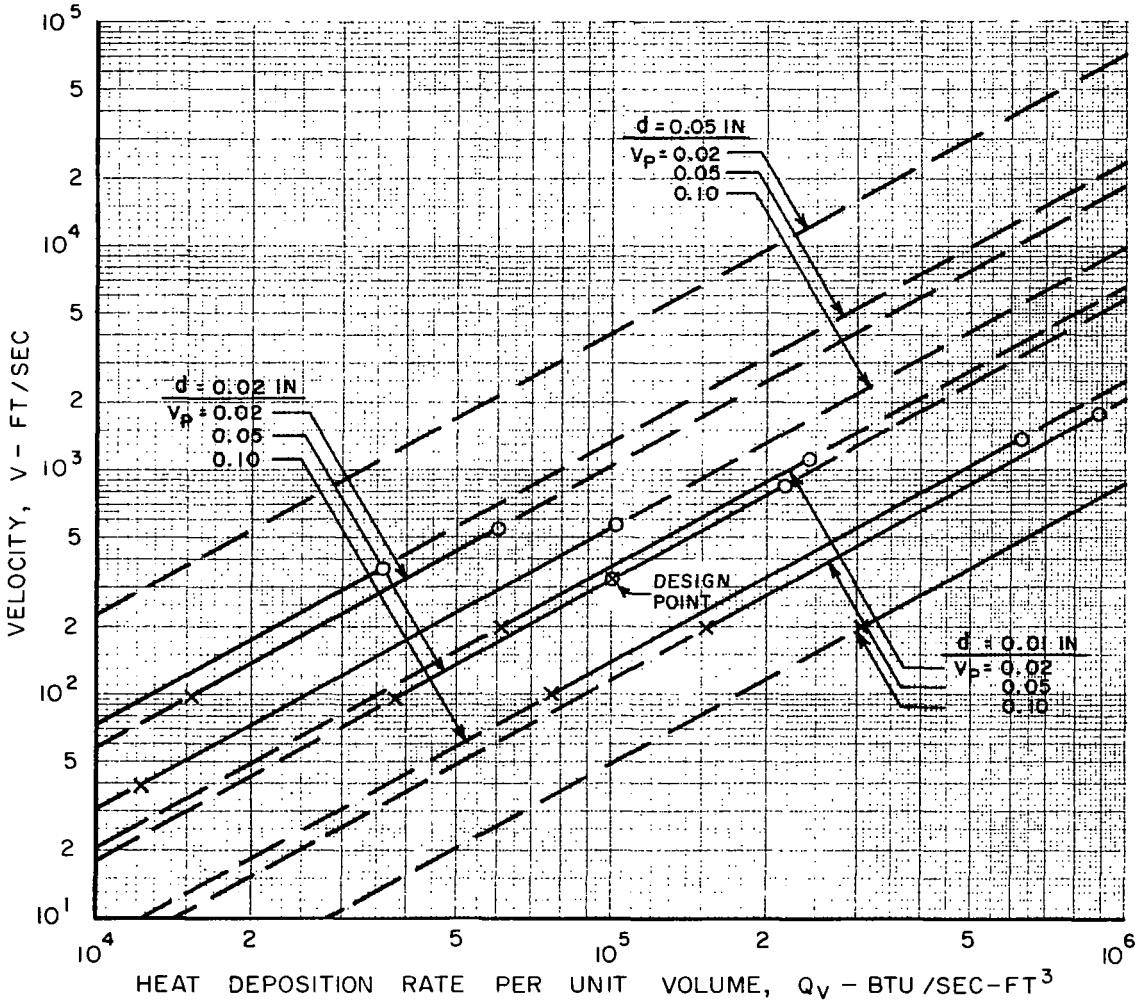

EFFECT OF HEAT DEPOSITION RATE IN MODERATOR ON DYNAMIC PRESSURE IN COOLANT PASSAGES

TEMPERATURE DIFFERENCE, $T_W - T_C$ = 200 R

COOLANT TEMPERATURE GRADIENT, $\Delta T_C/\Delta X$ = 6000 R/FT

HYDROGEN TEMPERATURE, T_C = 4000 R

HYDROGEN PROPERTIES GIVEN IN TEXT

PRESSURE = 1000 ATM (DYNAMIC PRESSURE INVERSELY PROPORTIONAL TO GAS PRESSURE)

× INDICATES REYNOLDS NUMBER OF 5000

○ INDICATES $T_{W_M} - T_W$ = 500 DEG R (SEE FIG. 17)

$$q = \frac{1}{0.00514\, g\, \rho}\ \frac{d^3 Pr^{5/3}}{\mu^{0.50}}\ \left(\frac{Q_V}{V_P C_P (T_W - T_C)}\right)^{2.5} \qquad \text{EQ. (17)}$$

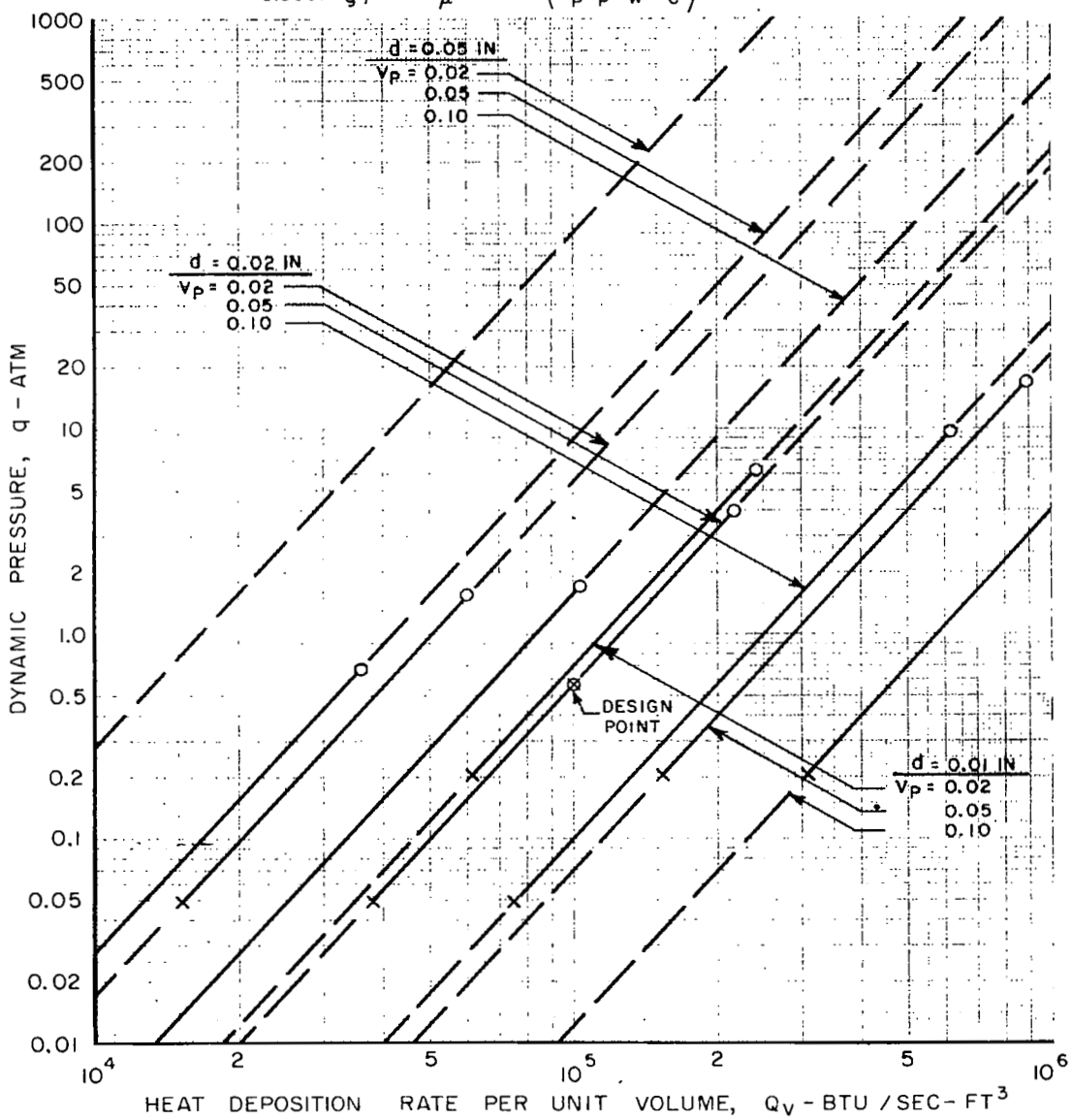

Figure 24

EFFECT OF HEAT DEPOSITION RATE IN MODERATOR ON PRESSURE GRADIENT IN COOLANT PASSAGES

TEMPERATURE DIFFERENCE, $T_W - T_C$ = 200 R

COOLANT TEMPERATURE GRADIENT, $\Delta T / \Delta X$ = 6000 R/FT

HYDROGEN TEMPERATURE, T_C = 4000 R

HYDROGEN PROPERTIES GIVEN IN TEXT

PRESSURE = 1000 ATM (PRESSURE GRADIENT INVERSELY PROPORTIONAL TO PRESSURE)

× INDICATES REYNOLDS NUMBER OF 5000

○ INDICATES $T_{W_M} - T_W$ = 500 DEG R (SEE FIG. 17)

$$\frac{\Delta P}{\Delta X} = \frac{d^3 \, Pr^{7/3}}{0.00257 \, g \, \rho \, \mu^{0.50} \, (T_W - T_C)^{3.5}} \, \frac{\Delta T_C}{\Delta X} \left(\frac{Q_V}{V_P C_P} \right)^{2.5} \qquad \text{EQ.(20)}$$

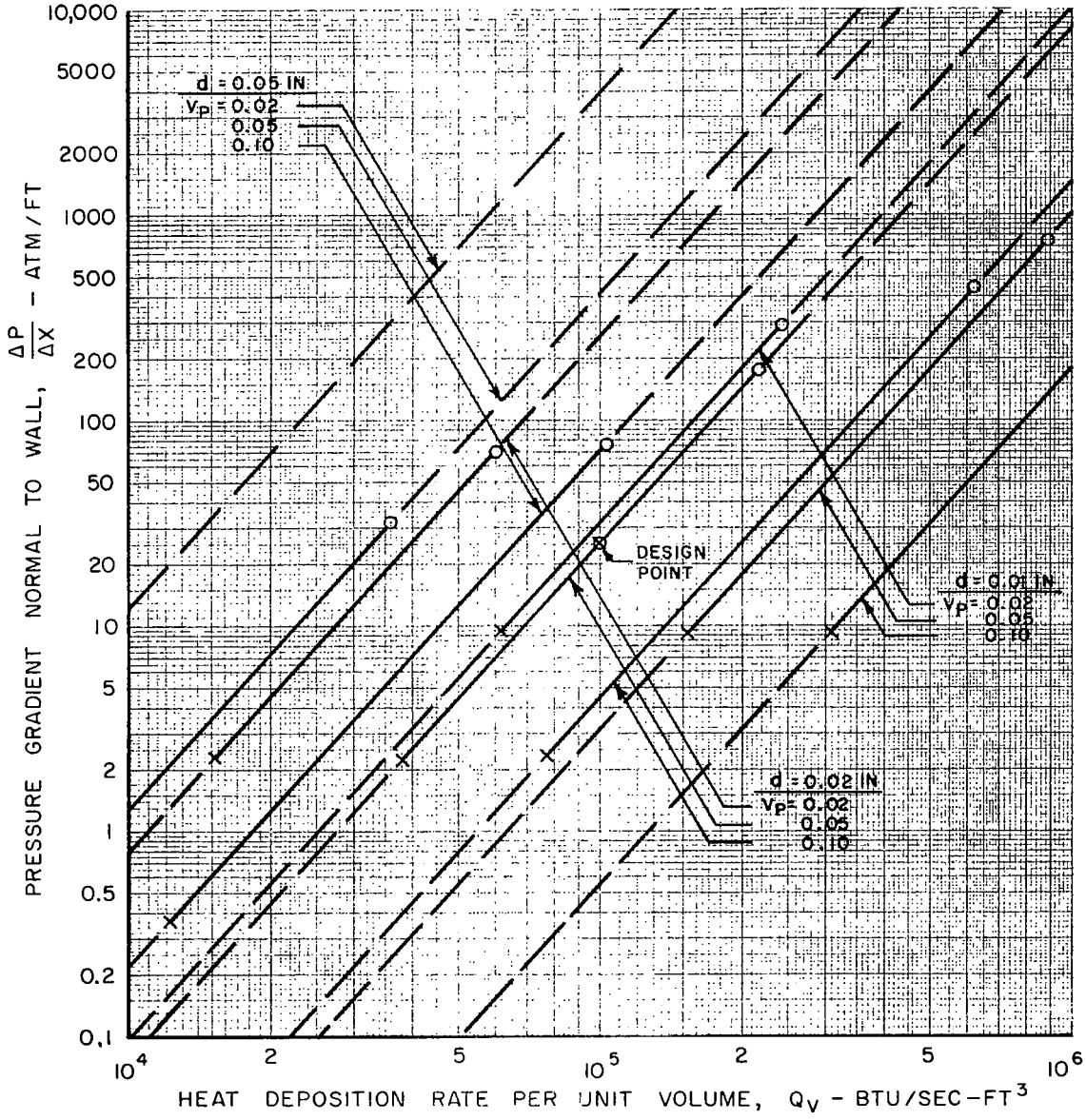

EFFECT OF COOLANT PASSAGE VOLUME FRACTION ON PRESSURE GRADIENT IN COOLANT PASSAGES

HEAT DEPOSITION RATE, $Q_V = 10^5$ BTU/SEC-FT^3
COOLANT TEMPERATURE GRADIENT, $\Delta T_C/\Delta X = 6000$ R/FT
HYDROGEN TEMPERATURE, $T_C = 4000$ R
HYDROGEN PROPERTIES GIVEN IN TEXT
PRESSURE = 1000 ATM (PRESSURE GRADIENT INVERSELY PROPORTIONAL TO PRESSURE)
$\Delta T = T_W - T_C$
× INDICATES REYNOLDS NUMBER OF 5000
○ INDICATES $T_{W_M} - T_W = 500$ DEG R (SEE FIG. 17)

$$\frac{\Delta P}{\Delta X} = \frac{d^3 P_r^{7/3}}{0.00257\, g \rho \mu^{0.50} (T_W - T_C)^{3.5}} \frac{\Delta T_C}{\Delta X} \left(\frac{Q_V}{V_P C_P}\right)^{2.5} \qquad \text{EQ (20)}$$

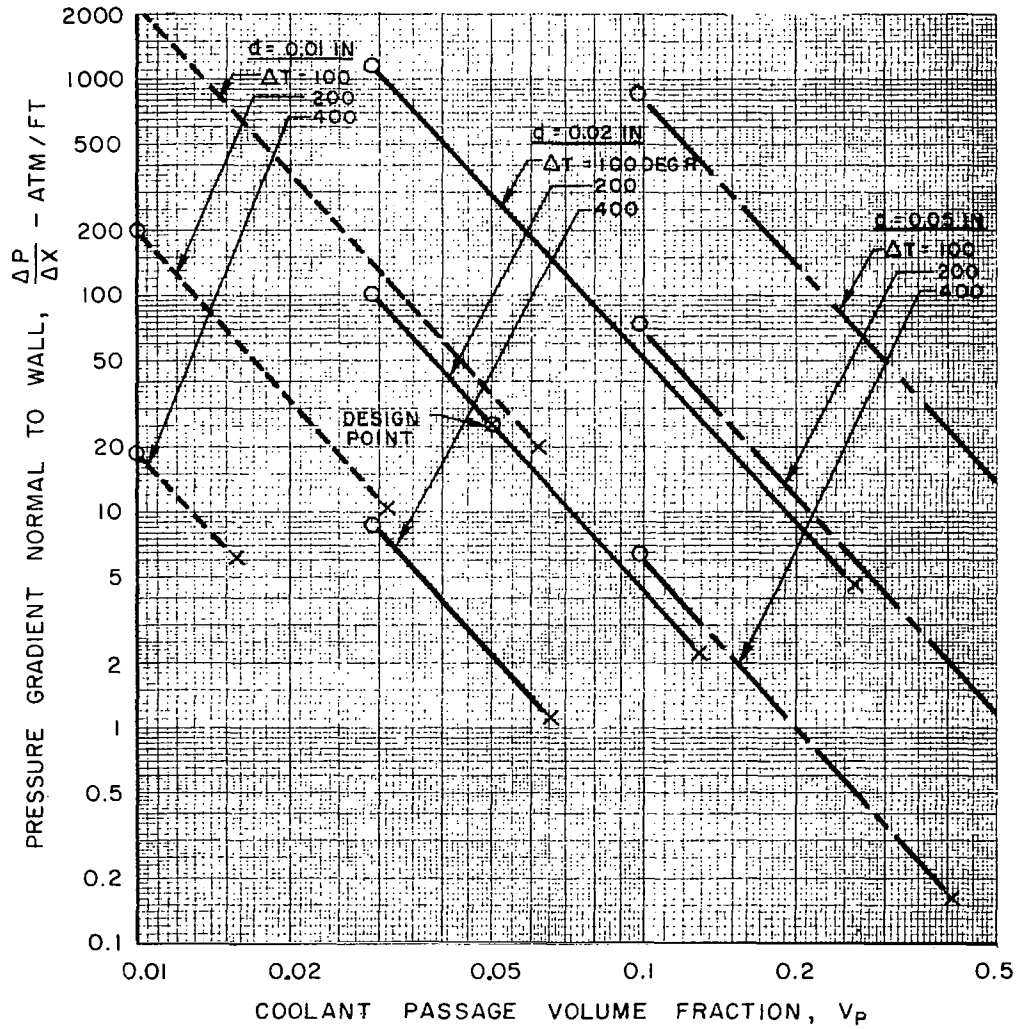

Figure 26

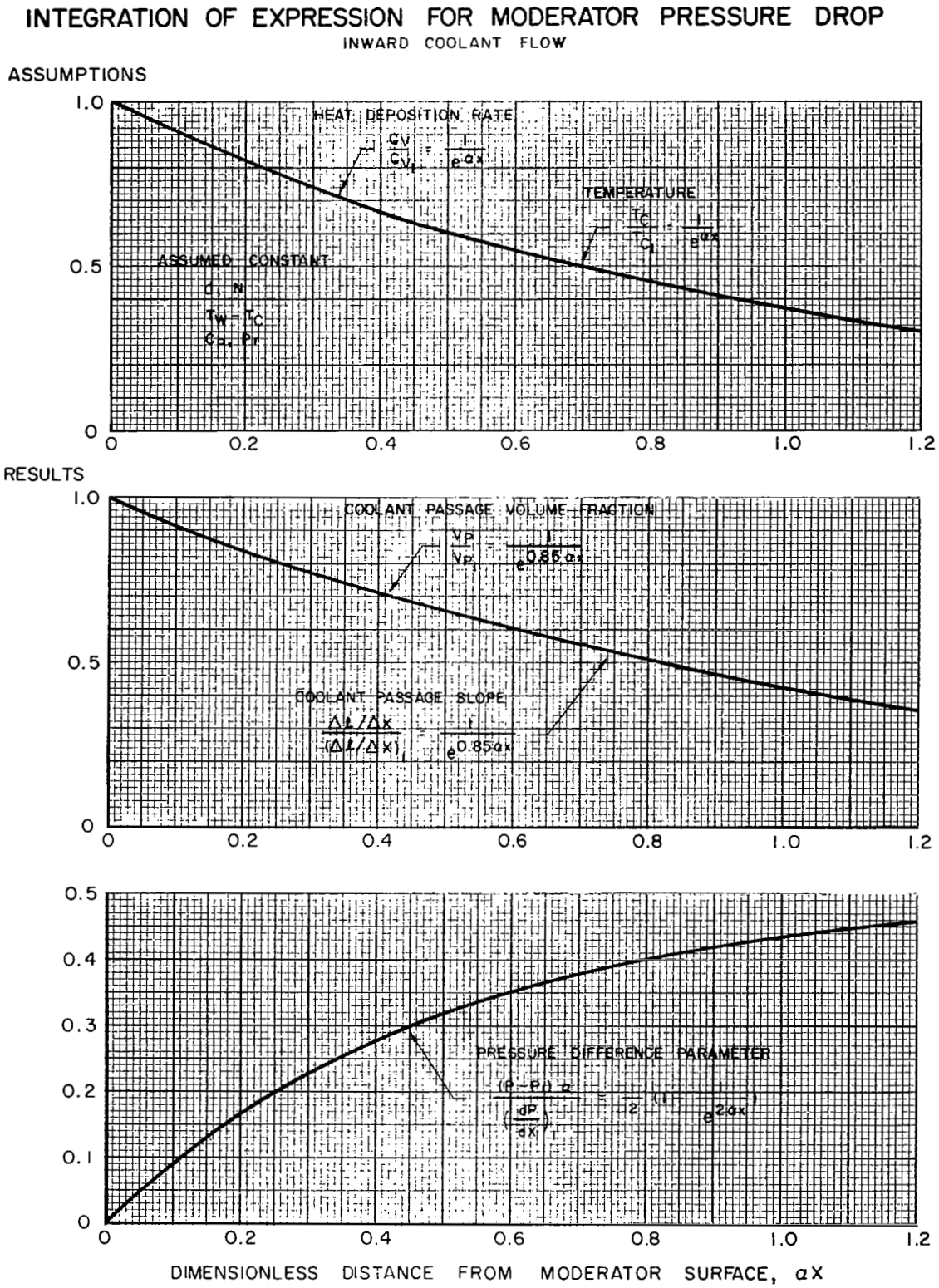
INTEGRATION OF EXPRESSION FOR MODERATOR PRESSURE DROP
INWARD COOLANT FLOW
ASSUMPTIONS
HEAT DEPOSITION RATE
ASSUMED CONSTANT
TEMPERATURE
RESULTS
COOLANT PASSAGE VOLUME FRACTION
COOLANT PASSAGE SLOPE
PRESSURE DIFFERENCE PARAMETER
DIMENSIONLESS DISTANCE FROM MODERATOR SURFACE, αX

VARIATION OF HYDROGEN PROPERTIES WITH DISTANCE IN FIZZLER NUCLEAR ROCKET

P_H = 500 ATM

FIZZLER ROCKET DEFINED SUCH THAT RATIO OF FUEL DENSITY TO PROPELLANT DENSITY (HYDROGEN DENSITY) IS INDEPENDENT OF POSITION

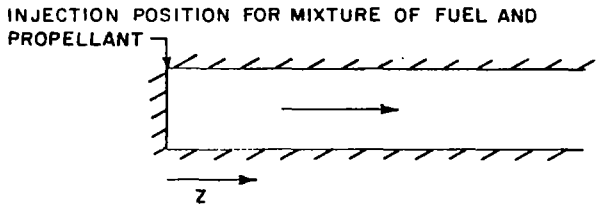

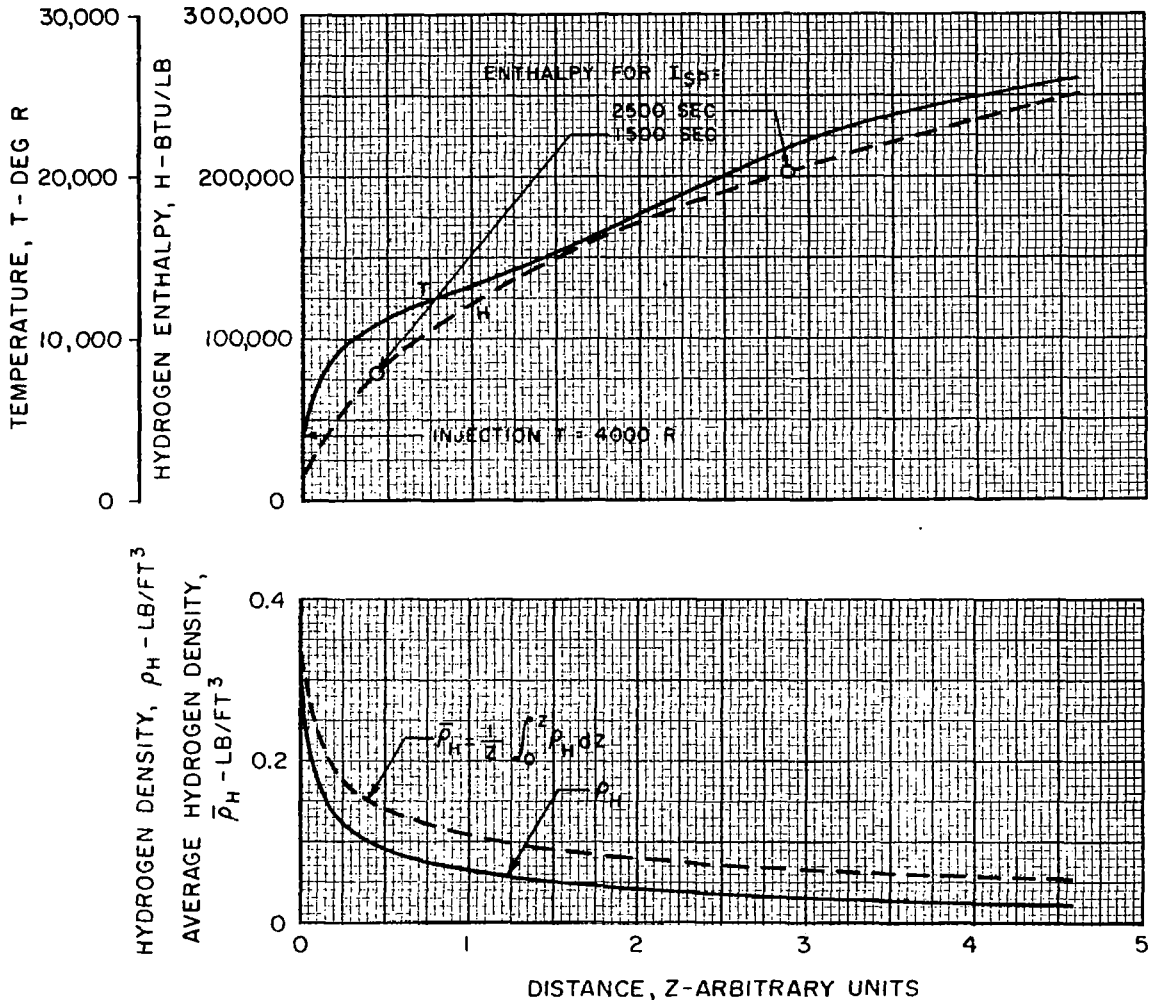

Figure 28

RATIO OF HYDROGEN FLOW TO FUEL FLOW IN FIZZLER NUCLEAR ROCKET

FUEL DENSITIES FOR NUCLEAR CRITICALITY FROM REF. 19
SPECIFIC IMPULSE (NEGLECTING EFFECT OF FUEL DENSITY)

— — — I_{SP} = 1500 SEC
——— 2500

NOTE: $\frac{W_H}{W_F} = \frac{\bar{\rho}_H}{\bar{\rho}_F}$ FOR CRITICALITY, REF. 19

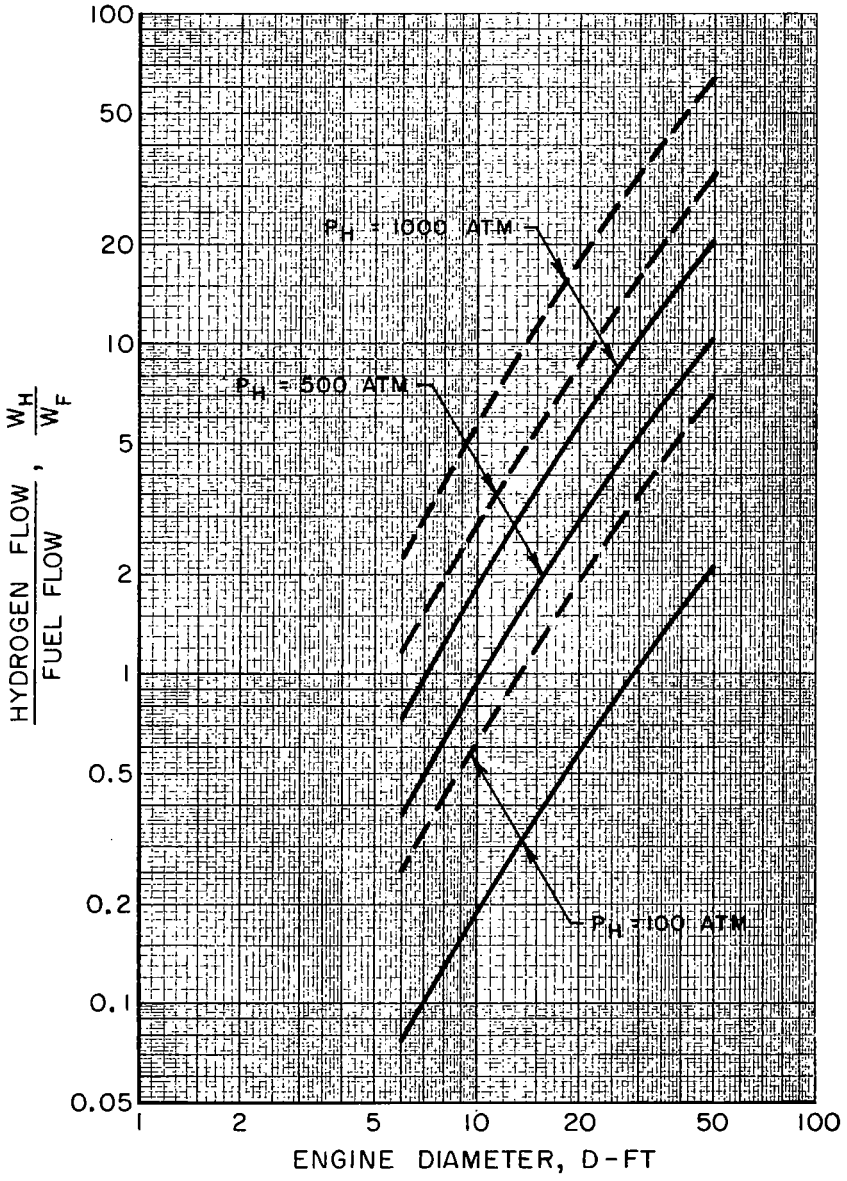

EFFECT OF SPACE RADIATORS ON SPECIFIC IMPULSE AND OVERALL THRUST-TO-WEIGHT RATIO OF HYDROGEN AND WATER ROCKETS

RADIATOR TEMPERATURE, DEG R	ASSUMED RADIATOR WEIGHT		
	LB/FT^2	$\frac{\text{LB}}{\text{BTU/SEC}}$	LB/KW
2000	1.0	0.130	0.123
4000	1.0	0.00813	0.00772
6000	1.0	0.00161	0.00153

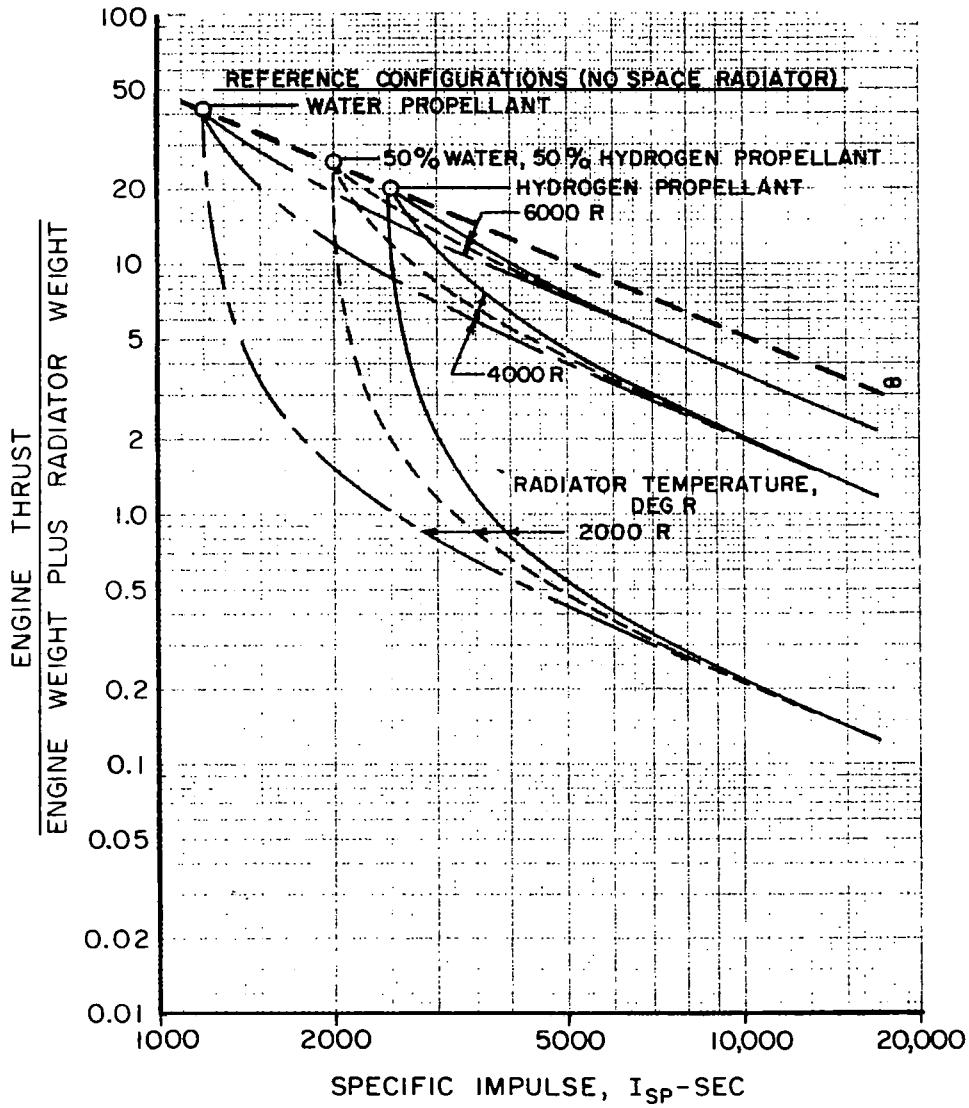

Figure 30

PRINCIPLE OF OPERATION OF FACILITY FOR TESTING GASEOUS NUCLEAR ROCKETS

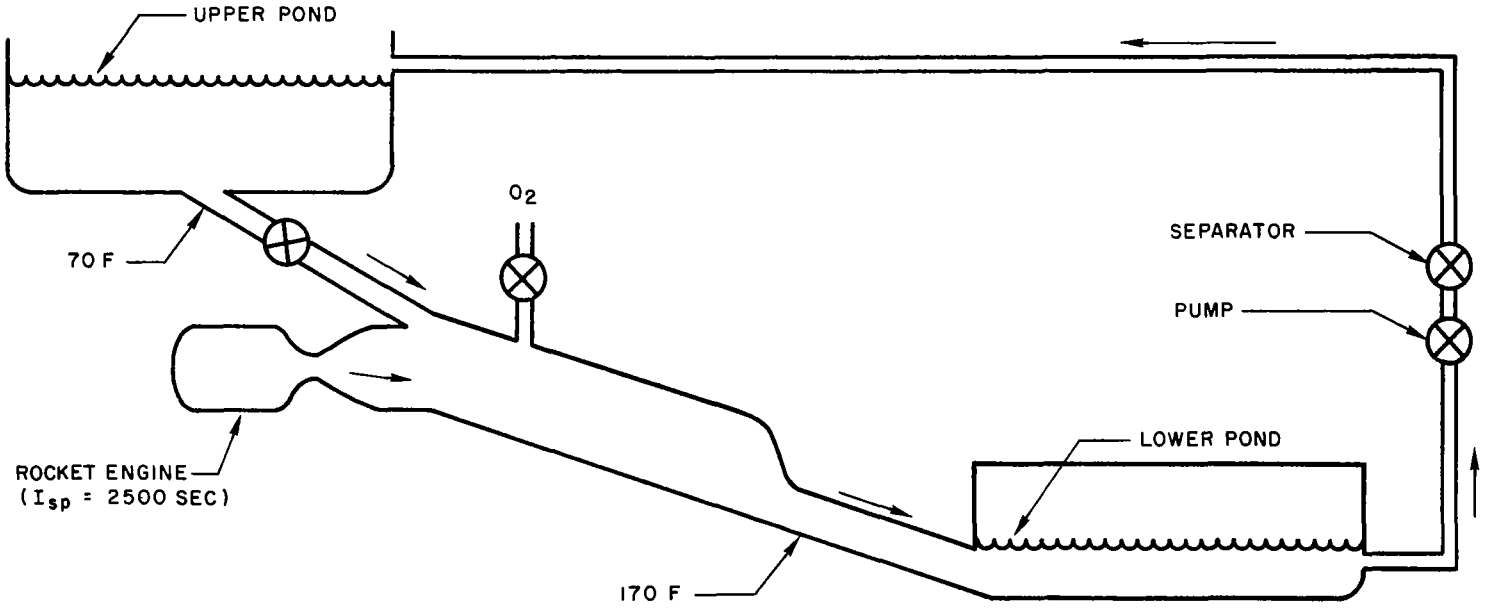

PROPELLANT (FLOW = 1 LB/SEC)	AUXILIARY INLET FLOW-LB/SEC		EXIT FLOW-FT3/SEC	
	O_2	H_2O	LIQUID	GAS
H_2	0	2000	32	230
	8	2500	40	0
CH_4	0	2000	32	29
NH_3	0	2000	32	0
H_2O	0	2000	32	0

NASA-Langley, 1965 CR-214